Classical Flt3L-dependent dendritic cells control immunity to protein vaccine

Niroshana Anandasabapathy,[1,2,6] Rachel Feder,[1,2] Shamim Mollah,[3] Sze-Wah Tse,[6] Maria Paula Longhi,[1,2] Saurabh Mehandru,[1,2] Ines Matos,[1,2] Cheolho Cheong,[1,2] Darren Ruane,[1,2] Lucas Brane,[1,2] Angela Teixeira,[1,2] Joseph Dobrin,[1,2] Olga Mizenina,[1,2] Chae Gyu Park,[1,2] Matthew Meredith,[2,4] Björn E. Clausen,[5] Michel C. Nussenzweig,[2,4] and Ralph M. Steinman[1,2]

[1]Laboratory of Cellular Physiology and Immunology, [2]Christopher H. Browne Center for Immunology and Immune Diseases, [3]Hospital Informatics, and [4]Laboratory of Molecular Immunology, The Rockefeller University, New York, NY 10065
[5]Institute for Molecular Medicine, University Medical Center of the Johannes Gutenberg-University Mainz, D-55131 Mainz, Germany
[6]Department of Dermatology/Harvard Skin Disease Research Center, Brigham and Women's Hospital, Boston, MA 02115

DCs are critical for initiating immunity. The current paradigm in vaccine biology is that DCs migrating from peripheral tissue and classical lymphoid-resident DCs (cDCs) cooperate in the draining LNs to initiate priming and proliferation of T cells. Here, we observe subcutaneous immunity is Fms-like tyrosine kinase 3 ligand (Flt3L) dependent. Flt3L is rapidly secreted after immunization; Flt3 deletion reduces T cell responses by 50%. Flt3L enhances global T cell and humoral immunity as well as both the numbers and antigen capture capacity of migratory DCs (migDCs) and LN-resident cDCs. Surprisingly, however, we find immunity is controlled by cDCs and actively tempered in vivo by migDCs. Deletion of Langerin$^+$ DC or blockade of DC migration improves immunity. Consistent with an immune-regulatory role, transcriptomic analyses reveals different skin migDC subsets in both mouse and human cluster together, and share immune-suppressing gene expression and regulatory pathways. These data reveal that protective immunity to protein vaccines is controlled by Flt3L-dependent, LN-resident cDCs.

CORRESPONDENCE
Niroshana Anandasabapathy: nanandasabapathy@partners.org

Abbreviations used: CCR7, C-C chemokine receptor type 7; cDC, classical DC; DT, diphtheria toxin; DTR, DT receptor; Flt3L, Fms-like tyrosine kinase 3 ligand; GLA-SE, glucopyranosyl lipid adjuvant-stable emulsion; migDC, migratory DC; polyIC(LC), polyinosinic-polycytidylic acid stabilized with polylysine double-stranded RNA and carboxymethylcellulose; ZBTB, zinc finger and BTB domain containing 46.

Human vaccines are delivered through skin, commonly by the s.c. route, allowing access to a rich network of DCs in skin and skin-draining LNs (Romani et al., 2010). s.c. injected vaccine antigens reach LNs that drain the skin and epithelial surfaces by passive transport through lymphatics or by DC antigen capture followed by subsequent cell-bound trafficking to the LNs, where T cell priming occurs (Itano et al., 2003). Resident DCs and several distinct migratory DC subsets (migDCs) that traffic to LN from skin are present in LNs (Förster et al., 1999; Henri et al., 2010b). The current paradigm is that both LN-resident DCs and migDCs have access to s.c. delivered antigen, are requisite, and cooperate to induce immunity (Itano et al., 2003; Allenspach et al., 2008). Based on this paradigm, vaccinology efforts have focused heavily on delivery of antigens to skin-resident DCs.

Flt3L is a DC hematopoietin that maintains DC numbers at set levels throughout adult life (Liu et al., 2007, 2009) and at sites relevant to vaccination, including the skin and skin-draining LN (Brasel et al., 1996; Maraskovsky et al., 1996). In healthy individuals, Flt3L is tightly regulated and at the limits of detection by ELISA; notably, it is 20-fold lower than CSF-1 or c-kit ligand (Shadle et al., 1989; Langley et al., 1993; Lyman and McKenna, 2003). Flt3L is secreted during acute infection, however, leading to DC-mediated support of NK function (Eidenschenk et al., 2010; Guermonprez, 2012). During s.c. immunization, the composition of DC subsets in the skin-draining LNs is transiently altered (Kastenmüller et al., 2011). It is unknown if Flt3L

Dr. Steinman died on 30 September 2011.

The Rockefeller University Press $30.00
J. Exp. Med. 2014 Vol. 211 No. 9 1875-1891
www.jem.org/cgi/doi/10.1084/jem.20131397

is secreted during immunization to regulate DC expansion acutely or if Flt3 signaling is required for productive immunity.

Flt3L and its receptor (Flt3, FLK2) instruct progenitors along a DC developmental pathway regulating the mobilization of preDCs from the blood to give rise to IFN-α–producing PDC, CD8α$^+$, and CD8α^{neg} cDCs in lymphoid organs and tissue-resident DCs such as Langerin$^+$CD103$^+$ DCs in skin (Waskow et al., 2008). Lymphoid CD8α$^+$ (Bozzacco et al., 2010) and tissue CD103$^+$ DCs both cross-present antigens (the major pathway of tumor and viral antigen presentation), derive from preDCs (Ginhoux et al., 2009), and share Flt3L developmental dependence (Liu et al., 2009), with common regulation downstream of Flt3 by mTOR (Sathaliyawala et al., 2010). These findings suggest DC ontogeny may dictate function, one rationale for the use of hematopoetins to selectively drive DC development for clinical use. Flt3L is being reintroduced to the clinic to potentiate human vaccines. It is unclear if bias by Flt3L to cross-presenting DCs from skin and LN may be exploited for protein-based vaccine delivery. Also, Langerin$^+$ CD103$^+$ DCs, which are tissue-resident migDCs originating from skin, are specialized to cross-present viral antigens to T cells during cytolytic infection (Bedoui et al., 2009a). However, their role in immunization to viral antigens has not been established.

We observe Flt3 is required for robust immunity to s.c. immunization and can enhance immunity. Surprisingly, we find that irrespective of Flt3L treatment, migDCs in the LN (including Langerin$^+$ CD103$^+$ cross-presenting DCs) are not required for CD4$^+$ T cell effector function, despite having greater efficiency of s.c. protein capture in the LN than resident CD8α cDCs. Impairing DC migration from skin to the sdLN via knockout of the CCR7 receptor and deletion of migDC subsets including Langerin$^+$CD103$^+$ DCs enhanced, not diminished, immune priming. Rather, the immune response develops through CD11c$^+$ ZBTB46-dependent cDCs. Transcriptomics in mouse and human reveal migDC subsets from skin relate most closely to each other and share gene signatures related to dampening of DC and T cell activation. Thus, we demonstrate that the immune response is controlled by cDCs in lymphoid tissue and that tissue microenvironment may confer immunosuppressive DC function in vivo.

RESULTS

s.c. immunity is Flt3L dependent

To assess if Flt3L is detected after immunization, we compared serum murine Flt3L levels by ELISA before and after immunization with adjuvant and a vaccine that targets protein antigens to DCs in vivo using antibodies directed against the C-type lectin CD205. Elevated Flt3L was detected in serum within 1 h of administering adjuvant with 0.5 µg of HIV gag p24-αCD205 fusion antibody (αCD205-gag p24; Fig. 1 A). As adjuvant, we tested both GLA-SE (glucopyranosyl lipid adjuvant-stable emulsion), which acts through TLR4 (Duthie et al., 2011; Pantel et al., 2012), and the adjuvant polyIC(LC) (polyinosinic-polycytidylic acid stabilized with polylysine double-stranded RNA and carboxymethylcellulose), which is a double-stranded DNA mimic that signals through TLR3 (Schulz et al., 2005) and MDA5 (Gitlin et al., 2006). To assess if Flt3 signaling was required, we compared prime-boost immunization with 0.5 µg αCD205-gag p24 vaccine with GLA-SE in control versus Flt3$^{-/-}$ mice. Flt3$^{-/-}$ mice consistently had 50% lower vaccine responses (Fig. 1 B). Collectively, these data suggest Flt3L is secreted after adjuvant administration with protein immunization and Flt3 signaling is required for optimal immunity.

To assess the impact of Flt3L on s.c. immunization, we treated mice with Flt3L or PBS surrounding prime-boost immunization with GLA-SE (Fig. 1 C). Upon antigen recall, we observed markedly increased IFN-γ production in CD4$^+$ T cell isolated from spleen when challenged with HIV-gag p24, but not control p17 peptides (Fig. 1 D and Fig. S1, gating). Flt3L-treated mice had enhanced antigen-specific clonal expansion in vitro (CFSE^{low}, IFN-γ$^+$) and enhanced CD4 T cell IFN-γ responses ex vivo when isolated from draining LNs, lung parenchyma, and small intestinal lamina propria as assayed by intracellular cytokine staining (ICS). Improved titers of serum IgG directed against gag p24 were observed. To determine if Flt3L-improved protein immunization is adjuvant specific, we also tested polyIC(LC) as adjuvant (Fig. 1 E). We again observed enhanced CD4 IFN-γ recall, CD4$^+$ clonal expansion, mucosal immunity, and HIV gag p24-specific IgG titers.

To determine if Flt3L potentiates both soluble and DC-targeted protein vaccines, we immunized mice with soluble versus αCD205-targeted gag p24 and GLA-SE. Flt3L improved soluble and DC-targeted responses (Fig. 2 A). At high antigen dose (5 µg) irrespective of Flt3L treatment, no difference was observed when comparing soluble to targeted vaccine responses. However, at 0.5 µg, antibody-mediated antigen targeting imparted a significant benefit to immunization. This effect was not dose-sparing, as targeted vaccination irrespective of Flt3L treatment resulted in improved clonal proliferation with respect to soluble antigen (Fig. 2 B). Similar trends were noted in mucosa and LNs (unpublished data). Thus, Flt3L improves both DC-targeted and nontargeted protein immunization. We established that targeting specificity through αCD205 occurred at 0.5 µg as soluble protein immunization lacked a discernible response at 0.5 µg (Fig. 2, A and B).

Although αCD205-gag p24 priming in primates induces both CD4 and CD8 immunity, in B6 mice we observe only CD4$^+$ priming due to epitope restriction (Trumpfheller et al., 2008). To assess Flt3L treatment on cross-presentation to CD8$^+$ T cells, we examined polyclonal CD8$^+$ T cell responses after immunization to αCD205-OVA with polyIC(LC). CD8$^+$ T cell IFN-γ was assayed using mixed OTI and II recall peptides and p24-pooled peptide controls. When assayed from lung parenchyma, spleen, and lamina propria, T cells from Flt3L mice had increased CD8$^+$ T cell IFN-γ production, proliferation, and IgG titers to OVA (Fig. 2 C). Therefore, we conclude Flt3L enhanced cross-presentation to CD8$^+$ T cells.

Flt3L expands CD205$^+$ LN-resident cDCs and migratory DCs and enhances in vivo αCD205-based antigen capture

To better understand the possible mechanisms underlying Flt3L enhancement of s.c. immunization, we examined the effect of

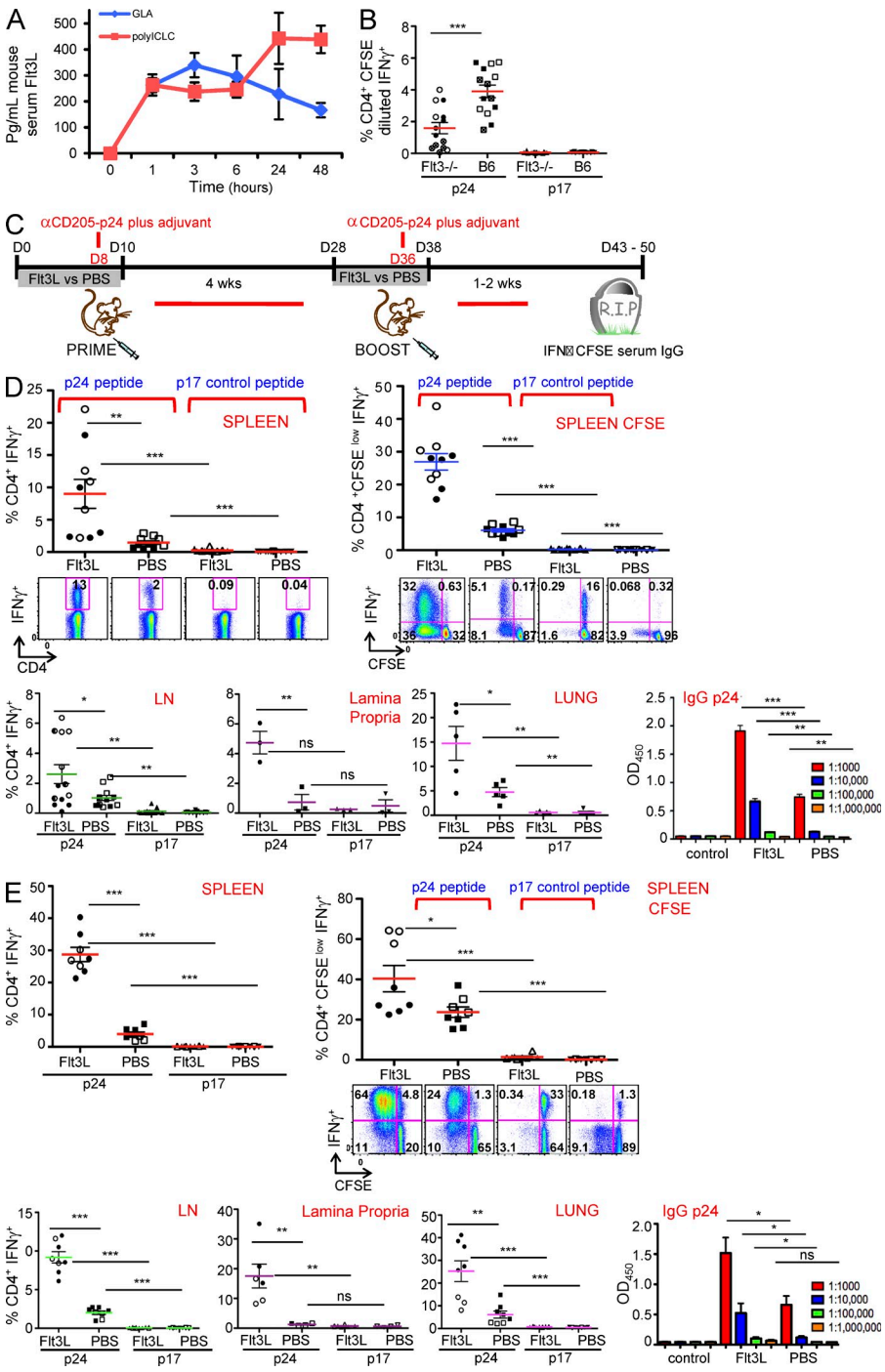

Figure 1. s.c. immunity is Flt3L dependent. (A) Serum from $n = 3$–5 mice taken before (0 h) or at 1, 3, 6, 24, or 48 h after s.c. immunization with 0.5 µg of αCD205 gag-p24 and GLA (blue) or polyIC(LC) (red). Error bars show mean ± SD. (B) CD4+ IFN-γ+ intracellular cytokine staining from 3 pooled experiments of 4–5 individual WT versus Flt3$^{-/-}$ mice after s.c. vaccination with GLA + 0.5 µg αCD205 gag-p24. Open, filled, and patterned symbols depict individual experiments. Error bars show mean ± SEM ($P \leq 001$). (C) Schematic of vaccine immunization schedule and Flt3L versus PBS treatment. (D) CD4+ T cell immunity at lymphoid and mucosal sites and humoral immunity after protein immunization to HIV-gag with multiple adjuvants: GLA (D) and polyIC(LC) (E). CD4+ IFN-γ+ intracellular cytokine staining from splenocytes of individual mice s.c. vaccinated with adjuvant + 5 µg αCD205 gag-p24 in spleen, LN, lamina propria, and lung. CD4+ IFN-γ+ + CFSE divided T cells after 96 h from individual immunized mice depicted in spleen. Circles represent individual mice, open versus filled (pooled from 2 independent experiments, 3–5 mice per group). Error bars show mean ± SEM. *, $P \leq 0.05$; **, $P \leq 0.01$; ***, $P \leq 0.001$. Gag-p24 serum total IgG in Flt3L-treated versus untreated mice, mean ELISA OD_{450}, unimmunized controls. Error bars show mean ± SEM across 5 individual mice from 1 representative experiment. *, $P \leq 0.05$; **, $P \leq 0.01$; ***, $P \leq 0.001$.

Flt3L on DC subsets in the skin-draining LNs of Flt3L-treated, control, and Flt3L$^{-/-}$ mice (Fig. S2, A and B, gating). Flt3L markedly increased PDCs and cDCs in skin-draining LNs (Fig. 3, A and B). PDCs are CD205^{-} and PDCA1^{+} (unpublished data). Within cDCs, we observed consistent expansion of CD8α^{+} CD11b^{low} and CD8α^{neg} CD11b^{high} cDC numbers. CD205^{+} CD8α^{+} DCs comprise ∼40% of CD8α^{+} cDCs in the skin-draining LNs. Upon Flt3L treatment, CD205^{+} CD8α^{+} cDCs cells were enriched to 73% of cDCs (Fig. 3 B; cell surface and intracellular CD205 staining). In vitro CD8α cDC capture of CD205 was almost 100% efficient at 1 and 3 h, and the percentage of cDCs that captured αCD205 in vitro was increased by Flt3L due to higher representation of this population (Fig. 3 C; from 44 to 67%). This corresponded closely to the shift in total percentage of CD205^{+} cells (Fig. 3 B). Flt3L also contributed to an overall expansion of total migDCs.

Five phenotypically distinct migDC populations traffic from skin to draining LN (Henri et al., 2010a,b). Langerin^{+}

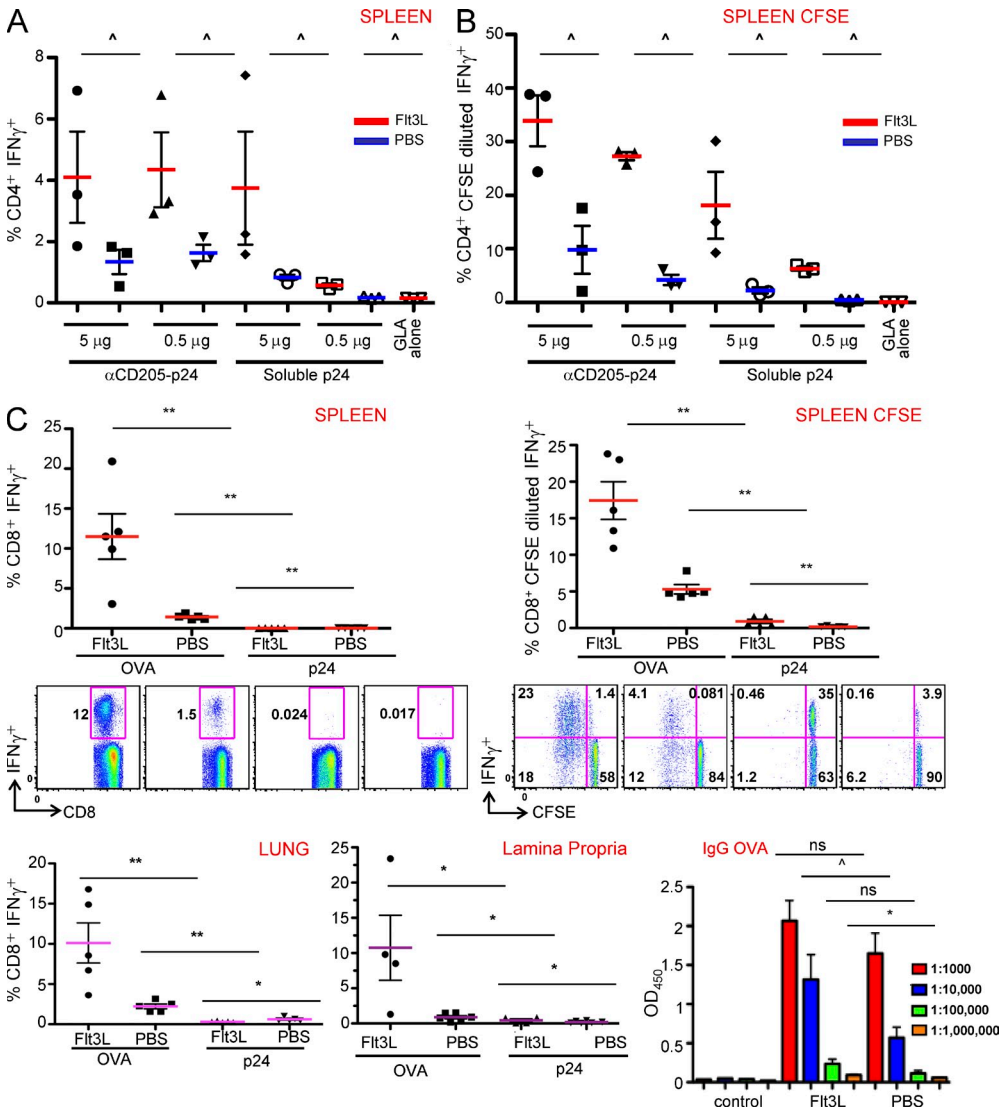

Figure 2. Flt3L potentiates both soluble and targeted vaccine priming and improves polyclonal CD8⁺ T cells responses and humoral immunity to OVA cross-presentation. Vaccine priming with αCD205-gag-p24 and soluble p24 at high (5 µg) and low (0.5 µg) doses in Flt3L-treated (red) versus PBS-treated (blue) mice. (A) Intracellular cytokine stain. (B) Proliferation of CD4⁺ T cells measured by CFSE-diluted IFN-γ⁺ cells. One representative experiment (n = 3 mice per group). Error bars show mean ± SEM. ^, P ≤ 0.1; *, P ≤ 0.05; **, P ≤ 0.01; ***, P ≤ 0.001. (C) CD8⁺ IFN-γ⁺ intracellular cytokine staining from individual mice vaccinated with polyIC(LC) + 5 µg αCD205 OVA intraperitoneal route in spleen, lung, and lamina propria (n = 4–6 mice pooled from 2 independent experiments). CD8⁺ IFN-γ⁺ CFSE low/divided T cells at 96 h. One of two representative experiments (n = 5). Error bars show standard error of the mean. CD8⁺ IFN-γ⁺ intracellular cytokine staining. OVA serum total IgG, mean ELISA OD_{450}. Error bars show mean ± SEM across 5 individual mice. ^, P ≤ 0.1; *, P ≤ 0.05; **, P ≤ 0.01; ***, P ≤ 0.001.

subsets include Langerhans cells (LCs), CD103⁺ Langerin⁺ dermal DCs, and the very rare CD103⁻ Langerin⁺ DCs. Langerin⁻ subsets include CD11b⁺ DCs and CD11b⁻ DCs. Although some increase in Langerin⁺ CD103⁺ DCs occurred after Flt3L treatment, we have observed the major expansion of migDCs was seen in the CD11b⁺ and CD11b⁻ compartment (Fig. 3 D; Mollah et al., 2014). Thus, Flt3L biases cDCs in the cutaneous LN toward CD8α CD205⁺ differentiation and expands migratory CD11b⁺, CD11b⁻, and CD103⁺ Langerin⁺ DCs. MigDCs express high levels of CD205⁺ (Fig. 3 D). After Flt3L treatment, a small decrease in in vitro capture of αCD205 by migDCs was apparent (from 75 to 69%; Fig. 3 E). To determine if migDCs and LN-resident cDCs in the nodes have equal access to antigen in vivo, we compared fluorescently labeled αCD205 capture 3 h after s.c. injection into Flt3L-treated and untreated mice (Fig. 3 F). MigDCs captured antigen with greater efficiency than cDCs by αCD205-A647 label in the proximal LNs (popliteal), irrespective of Flt3L treatment. Flt3L improved αCD205-A647 label by both migDCs in the distal LNs (inguinal) and cDCs in the proximal

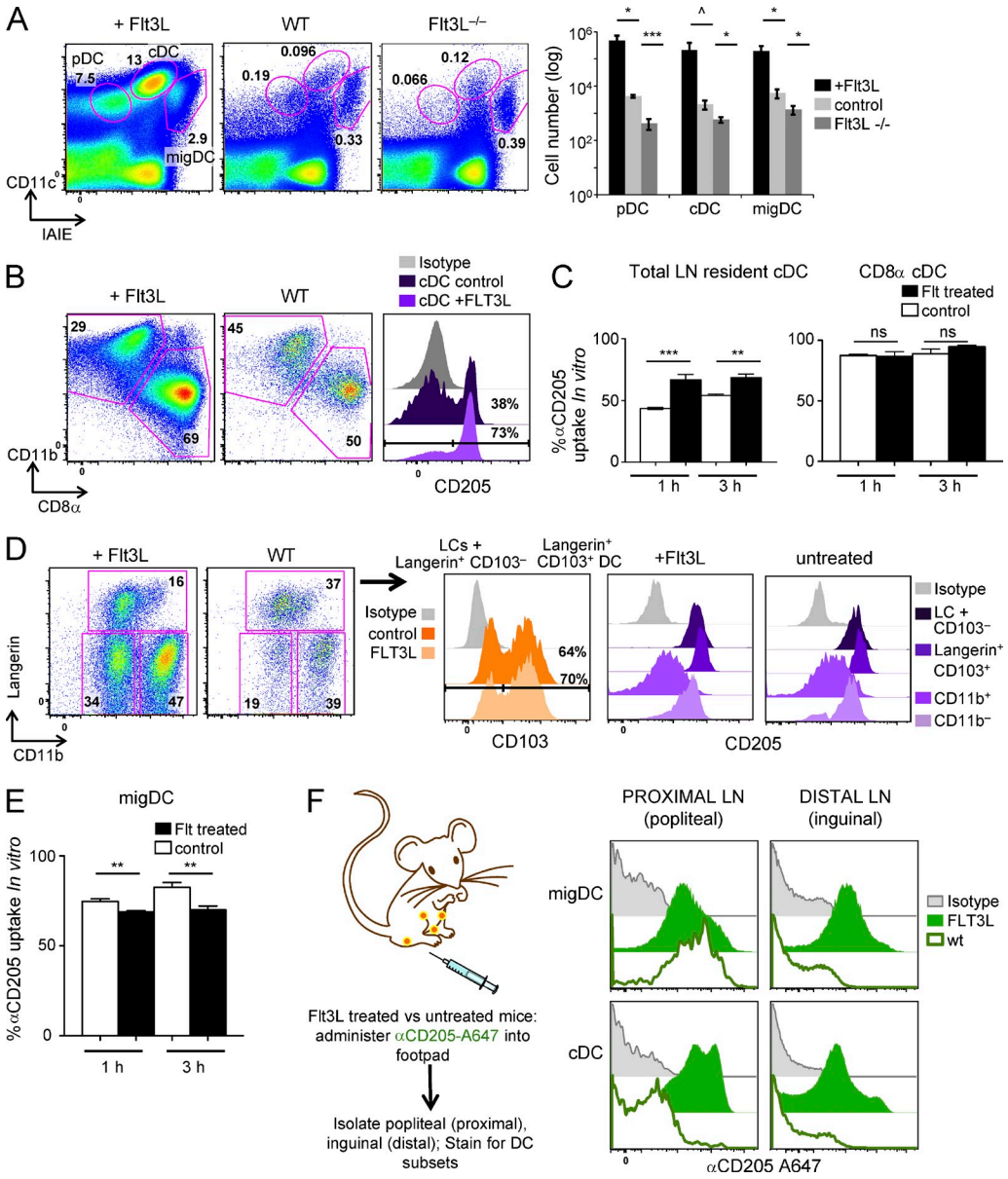

Figure 3. Flt3L expands classical, migratory, and plasmacytoid DC subsets in the skin draining LN and enhances antigen capture by CD205⁺ migratory and LN-resident cDCs in vivo. (A) Flt3L-treated (left) compared with WT (middle) and Flt3L$^{-/-}$ mice (right). One representative experiment (of three) with sample quantitation of DC subsets for two pooled skin-draining LNs. Error bars show standard deviation between 3 mice. ^, $P \leq 0.1$; *, $P \leq 0.05$; **, $P \leq 0.01$; ***, $P \leq 0.001$. (B) Representative CD8α⁺ CD11b low and CD8α⁻ CD11b high DC subset gating, from classical (cDCs) gate of skin draining LN from mice treated with Flt3L (left) or controls (right). Total % CD205 positive cells from within CD8α⁺ CD11b low cDC subset (cell surface and intracellular staining). (C) In vitro capture of αCD205 with equivalent total skin draining LN cells from Flt3L-treated versus PBS mice gated on total LN cDCs versus CD8α cDCs. One representative experiment of two with $n = 3$ mice per group, error bars depict SEM. *, $P \leq 0.05$; **, $P \leq 0.01$; ***, $P \leq 0.001$. (D) Skin draining LN migratory DC subsets from within IAIE^{hi} CD11c^{intermediate} population from mice treated with Flt3L (left) or controls (right). CD103⁺ gating from within Langerin⁺ subset. CD205 cell surface and intracellular staining from migratory subsets (flow cytometry). (E) In vitro capture of αCD205⁺ with equivalent total skin draining LN cells from Flt3L-treated versus PBS mice, gated on migDC. 1 representative experiment of 2 with $n = 3$ mice per group, error bars depict SEM. *, $P \leq 0.05$; **, $P \leq 0.01$; ***, $P \leq 0.001$. (F) αCD205-A647 versus Isotype-A647 control antibody was injected by s.c. immunization in the footpad of control versus Flt3L-treated recipients (n = three mice per group, one representative experiment of three, one representative FACS plot shown). At 3 h, draining (popliteal) versus distal (inguinal) LNs were harvested and migratory versus conventional DC subsets were gated for antibody uptake.

(popliteal) LNs (Fig. 3 F), suggesting improved antigen capture in vivo. Thus, in vivo migDCs in LNs captured and internalized αCD205 more rapidly than cDCs, and Flt3L improved antigen uptake by both.

s.c. immunization does not depend on Langerin⁺ DCs, including Langerin⁺ CD103⁺ DCs

Previous work suggested that migratory DCs initiate immune priming in the LN (Itano et al., 2003; Allenspach et al., 2008),

and we observed more rapid antigen capture by migDCs in LNs. Langerin 103$^+$ DCs are dermal migDCs that cross-prime to virus (Bedoui et al., 2009b), yet a role in viral vaccine priming has not been established. To address this, we used Langerin-diphtheria toxin (DT) receptor (DTR) mice (LDTR), where expression of the DTR in Langerin$^+$ cells permits depletion of Langerin$^+$ DCs by DT treatment (Noordegraaf et al., 2010). In LDTR mice, a single dose of DT leads to deletion in the skin-draining LN of some Langerin$^+$ CD8α^+ cDCs (Kissenpfennig et al., 2005), and all CD103$^+$ Langerin$^+$ dermal DCs and LCs (Bennett et al., 2005; Noordegraaf et al., 2010). Robust depletion of Langerin$^+$ migDCs occurred after DT administration in both untreated and Flt3L-treated mice including LC and CD103$^+$ migDCs (Fig. 4, A and B). DT was administered 3 d and 1 d before vaccination during prime and boost phases (schema, Fig. 4 C). At 5 μg of αCD205-gag p24 with adjuvant, all Langerin$^+$ DCs were dispensable for efficient vaccine priming at baseline, and their deletion did not diminish CD4$^+$ vaccine responses, irrespective of Flt3L treatment when compared with controls administered DT at the same dosing scheme. In some Flt3L-treated groups and in all PBS controls (LNs, Spleen), we were surprised to note significantly higher direct ex vivo effector responses in LDTR mice compared with WT controls as measured by CD4 IFN-γ production (Fig. 4, D and F).

Soluble protein immunization lacked a discernible IFN-γ or CFSE response at 0.5 μg when compared with adjuvant alone, establishing αCD205-targeted immune response specificity that occurred at 0.5 μg (Fig. 2 A). Under high antigen conditions, we reasoned that cDCs might capture excess antigen despite the loss of Langerin$^+$ populations. At 0.5 μg, s.c. immunization was likely not mediated through DCs in the spleen because splenectomized and control mice had equivalent responses (unpublished data). To test if Langerin$^+$ DCs were required for immunization under antigen-limiting doses, we also immunized DTR and control mice with 0.5 μg of αCD205-gag p24 and adjuvant (Fig. 4, D–H). We were surprised to note no loss of response occurred after DT treatment, suggesting that Langerin$^+$ DC subsets were not required, even under dose-limiting concentrations. Instead, we observed a trend that the immediate ex vivo IFN-γ response in LN, spleen, and lung was generally significantly higher upon ablation of Langerin$^+$ DCs (Fig. 4, D–F). In vitro CD4$^+$ proliferation to αCD205-p24 was not diminished in LDTR mice (Fig. 4 G). We also observed higher ex vivo IgG titers after deletion of Langerin$^+$ subsets, irrespective of Flt3L treatment, irrespective of both Flt3L and high (not depicted) or low antigen dose (Fig. 4 H). CD8$^+$ immunity to αCD205-OVA was preserved in Langerin-DTR versus B6 control mice treated with DT (Fig. 4, I–K) and a subtly heightened trend was again observed. This was probably not caused by enhanced antigen uptake by cDCs in LDTR versus control mice (Fig. 4 L). Collectively, these data suggest that Langerin$^+$ DCs, including LCs and Langerin$^+$ CD103$^+$ DCs, were dispensable to CD4 or CD8 T cell priming and greater ex vivo effector and humoral immunity to HIV gag was observed in the absence of Langerin$^+$ DCs.

Blockade of migratory DC entry to the LN enhances, not inhibits, s.c. and i.d. immunization

As described, steady-state migration of DCs from the skin to the draining LN depends on expression of the chemokine receptor CCR7. Mice that lack CCR7 demonstrate a complete absence of migDCs in the LN (Förster et al., 1999; Ohl et al., 2004) irrespective of Flt3L treatment (Fig. 5 A). To further address the contribution of migDCs to s.c. protein vaccination in the LN, we examined vaccine responses in CCR7$^{-/-}$ mice. This allowed us to test the contribution of all migDC subsets in the LN, including those that acquire antigen peripherally and traffic antigen to the LN, and those that have already arrived in the skin-draining LN at the time of antigen capture in the LN. Again, at both 5 and 0.5 μg of s.c. αCD205-gag p24 all migDCs were dispensable. (Fig. 5 B). Absence of migDCs in the skin-draining LNs of individual CCR7$^{-/-}$ mice compared with B6 control mice was confirmed at the time of harvest (Fig. 5 A and not depicted). Again, irrespective of Flt3L treatment we noted a trend of higher mean ex vivo CD4$^+$ IFN-γ responses in lymphoid organs and in tissue (spleen, LN, and lung) and in vitro recall T cell proliferation in CCR7$^{-/-}$ versus control mice. To ensure s.c. immunization did not bypass migratory DCs, we examined low-dose αCD205-gagp24 i.d. immunization into the flank (Fig. 5 C). Mice lacking CCR7 had significantly higher CD4$^+$ T cell IFN-γ levels in the draining proximal LN ($P < 0.0001$) and distally in spleen ($P < 0.05$) and nondraining LNs (unpublished data). These data suggested that blockade of CCR7-dependent DC migration to the LN enhances, not impairs, immunity.

To determine whether migratory DCs were requisite for CD8 immunity, we also tested s.c. αCD205-OVA immunization. Again, no loss of CD8$^+$ T cell proliferation in CCR7 KO mice was observed (Fig. 5 D). CCR7 KO mice may have defects in T reg cell activity that could support enhanced priming (Menning et al., 2007). To restrict CCR7 deficiency to DCs, we generated mixed bone marrow chimeras with CD45.1 and ZBTB46 DTR or CCR7 and ZBTB46DTR. Zbtb46 is a recently described cDC-specific transcriptional factor that distinguishes classical DCs from other mononuclear phagocytic lineages and from plasmacytoid DCs (Meredith et al., 2012; Satpathy et al., 2012). When uncompensated CCR7 loss was restricted to migDCs, there was no loss of immunity (Fig. 5 E). These mice could not be used to evaluate whether CCR7 deficiency in migDCs leads to increased immunity because ZBTB46 affects both tissue-resident and lymphoid-resident cDCs. Therefore, CCR7-dependent migratory DCs are not required for immunity.

ZBTB46-dependent cDCs are required for priming

To further clarify the cellular requirements for s.c. priming, we made BM chimeras comparing chimerization of control (CD45.1) BM to BM from several different DTR-expressing lines after DT treatment to deplete distinct cell populations. Chimerization was needed to avoid toxicity associated with DT administration directly to CD11c-DTR mice, although irradiated chimera recipients are older and generally have

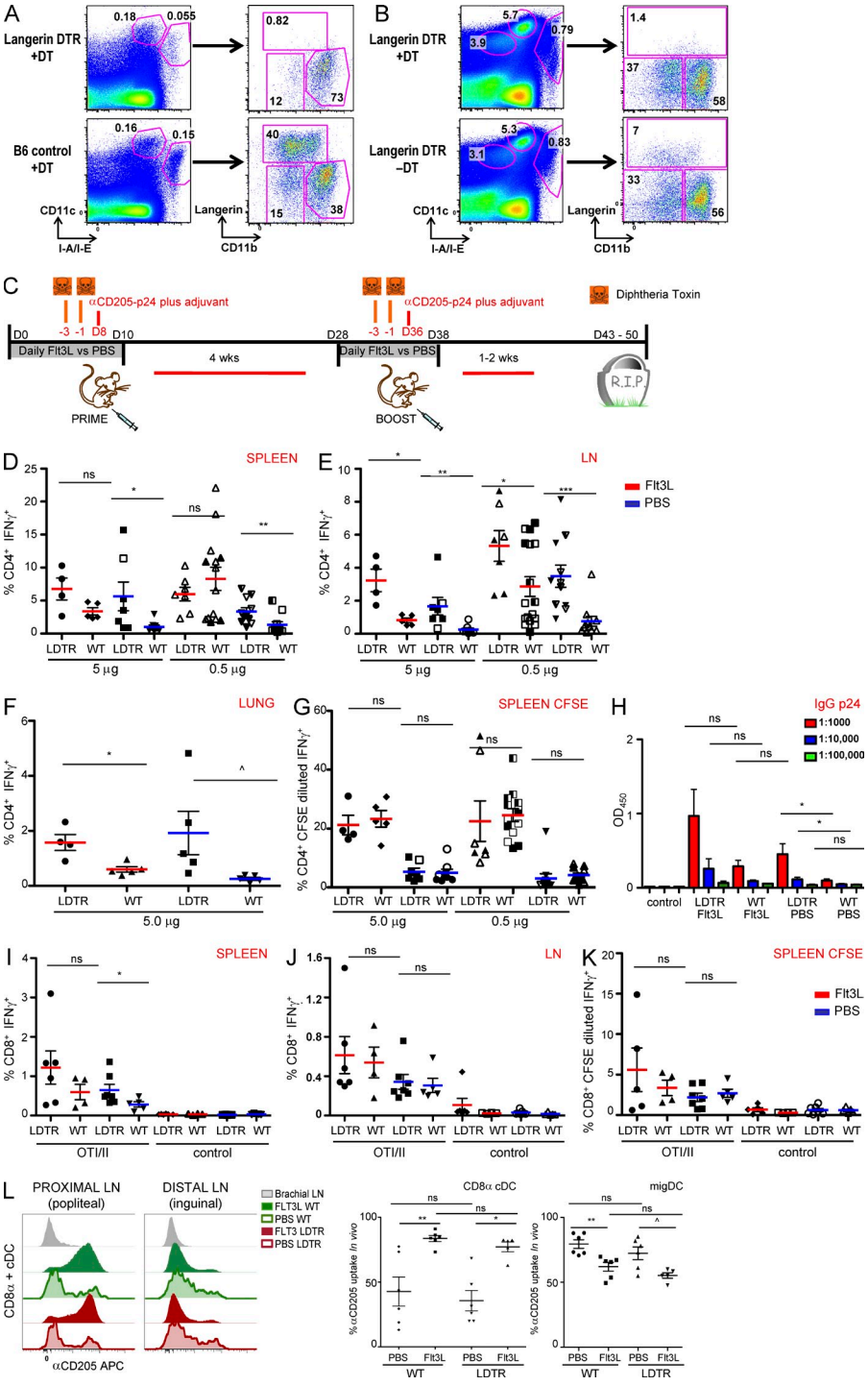

Figure 4. Langerin⁺ DC, including LCs and CD103⁺ DC, are not required for CD4 s.c. protein immunization. (A) Deletion of Langerin⁺ migratory DC subsets after a single dose (1 µg) DT administered 24 h before harvest. (B) Deletion of Langerin⁺ subsets in Flt3L-treated Langerin DTR mice administered Flt3L daily. DT was administered −3 and −1 d before harvest at day 8. (C) Schema: 1 µg DT was administered to Langerin DTR mice versus WT controls day −3 or −1 to s.c. vaccine prime or boost with GLA plus 5 or 0.5 µg αCD205 gag-p24. (D) Spleen, (E) LN, (F) Lung-intracellular cytokine staining. (G) CD4⁺ IFN-γ⁺ CFSE divided cells in Langerin DTR versus C57BL/6 WT mice in Flt3L-treated (red Flt3L treated, 1 representative experiment at 5 µg, or pooled from 2–3 independent experiments at 0.5 µg) or PBS-treated controls (blue, pooled from 2–3 independent experiments at 5 or 0.5µγ; ^, $P \le 0.1$; *, $P \le 0.05$; **, $P \le 0.01$; ***, $P \le 0.001$). (H) Serum HIV gag-p24 IgG titers in Langerin DTR versus WT mice treated with Flt3L versus PBS (one representative experiment of three ($n = 5$ mice), *, $P \le 0.05$, **, $P \le 0.01$, ***, $P \le 0.001$). (I–K) 1 µg DT was administered to Langerin DTR mice versus WT controls day −3 or −1 to vaccine prime or boost with s.c. polyIC(LC) plus 0.5 µg αCD205 OVA. In vitro challenge of OVA versus control peptide. (I) Spleen, (J) LN intracellular cytokine staining, and (K) CD8⁺ IFN-γ⁺ CFSE divided cells ($n = 4$–7 mice total per group pooled from 2 independent experiments). (L) Capture of αCD205 by classical CD8α⁺ LN cDCs 3 h after footpad injection (7.5 µg total) is improved by Flt3L but not altered after Langerin⁺ DC ablation. 1 µg of DT was administered at −3 and −1 d, with injection and harvest on day 0, after 9–10 d of PBS or Flt3L treatment. (left) WT (green), Langerin-DTR mice (red). (right) % αCD205uptake by cDCs and migDCs in the popliteal LNs. Pooled from two independent experiments ($n = 5$–6 mice total; ^, $P \le 0.1$; *, $P \le 0.05$; **, $P \le 0.01$; ***, $P \le 0.001$).

lower overall vaccine responses. We compared BM chimeras: CD45.1→CD45.2 (control), Langerin-DTR (L-DTR)→CD45.2, CD11c-DTR→CD45.2, and Zbtb46 DTR (Z-DTR)→CD45.2. IFN-γ T effector responses were impaired ex vivo in LN and spleen in Z-DTR and CD11c-DTR donor BM chimeras but not in L-DTR or CD45.1 controls with 0.5 µg of αCD205gag-p24 and GLA. The observed reduction was comparable to p17 controls (red vs. black; Fig. 6, A and B). A significant reduction in clonal expansion was observed after 4 d of culture in Z-DTR and in CD11c-DTR compared with control chimeras and littermate chimeras that had not received DT (Fig. 6 C, blue). In L-DTR chimeras, although radioresistant populations such as LCs were spared, radiosensitive Langerin⁺ CD103⁺ migDCs were deleted. Consistent with the observation that L-DTR unchimerized mice had heightened immunity, depletion of Langerin⁺ CD103⁺ DCs

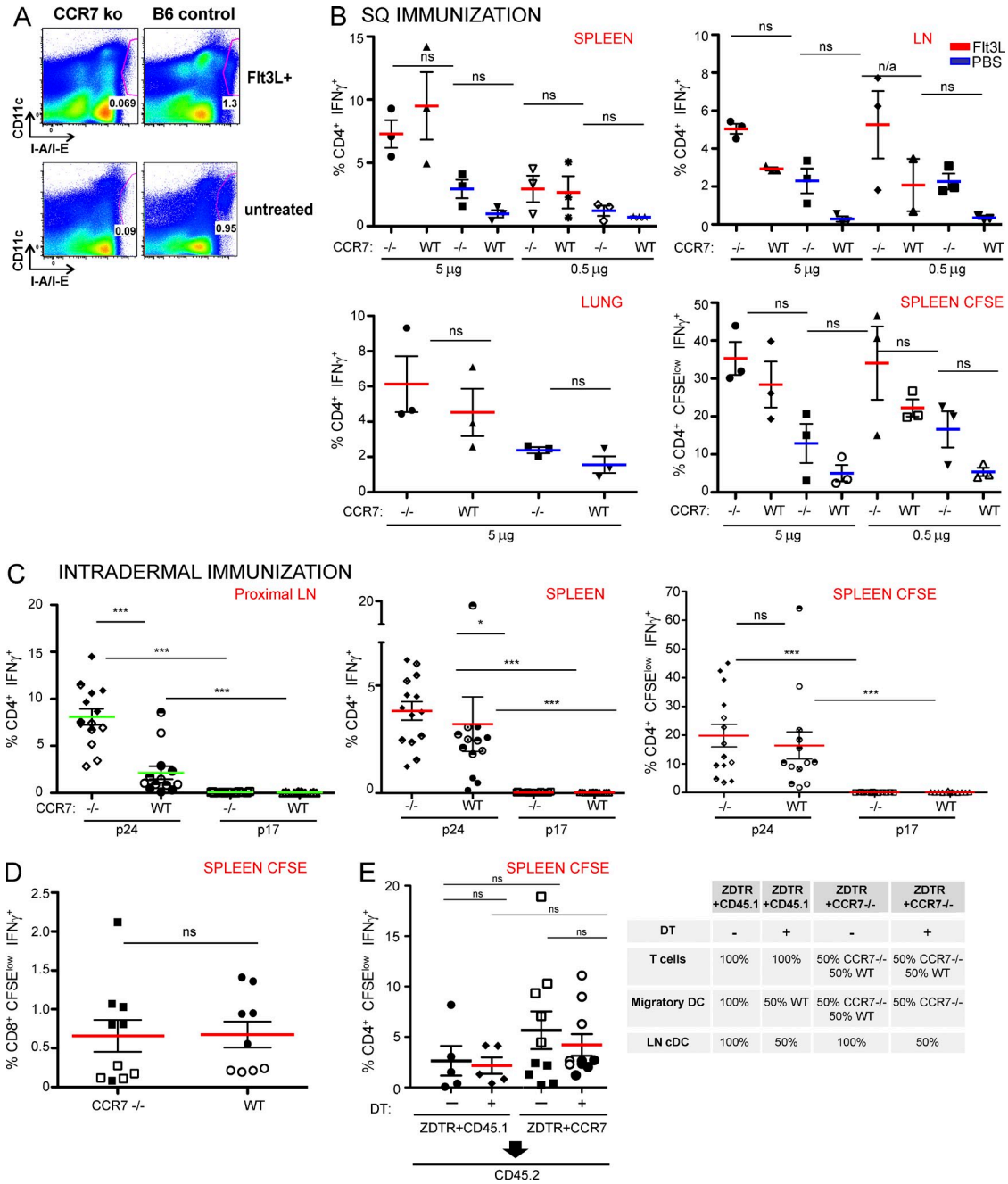

	ZDTR +CD45.1	ZDTR +CD45.1	ZDTR +CCR7-/-	ZDTR +CCR7-/-
DT	-	+	-	+
T cells	100%	100%	50% CCR7-/- 50% WT	50% CCR7-/- 50% WT
Migratory DC	100%	50% WT	50% CCR7-/- 50% WT	50% CCR7-/-
LN cDC	100%	50%	100%	50%

Figure 5. Blockade of migratory DCs does not impair immunity after s.c. or i.d. protein immunization. (A) Representative gating of inguinal LN taken from CCR7$^{-/-}$ and Flt3L-treated and untreated vaccine mice. (B) CCR7$^{-/-}$ mice versus B6 controls were immunized with 5 or 0.5 µg of αCD205 gag-p24 in separate experiments (n = 3 mice per group). Error bars show mean ± SEM. *, P ≤ 0.05; **, P ≤ 0.01; ***, P ≤ 0.001. Red, Flt3L treated; blue, PBS treated. Intracellular cytokine staining for spleen, LN, and lung parenchyma and CFSE dilution of splenocytes after 4 d in culture with p24. (C) i.d. immunization with 0.5 µg αCD205 gag-p24: proximal draining LN and spleen intracellular cytokine staining and CFSE dilution of splenocytes after 4 d in culture with p24. Pooled from 3 independent experiments of n = 5 mice per group. Error bars show mean ± SEM. *, P ≤ 0.05; **, P ≤ 0.01; ***, P ≤ 0.001). (D) CD8$^+$ CFSE divided IFN-γ T cells after DEC-OVA SQ immunization. Pooled from 2 experiments, n = 4–5 mice per group. Error bars show mean ± SEM. *, P ≤ 0.05; **, P ≤ 0.01; ***, P ≤ 0.001. (E) Mixed bone marrow chimera after SQ immunization with 0.5 µg αCD205 gag-p24 in the presence or absence of DT, CFSE dilution shown. Pooled from 2 independent experiments with n = 4–5 mice per group for CCR7$^+$ZDTR chimeras compared plus and minus DT; n = 1 experiment for 5 mice per group for CCR7$^+$CD45.1 plus and minus DT controls. Error bars show mean ± SEM. *, P ≤ 0.05; **, P ≤ 0.01; ***, P ≤ 0.001.

in L-DTR chimeras produces heightened ex vivo CD4$^+$ immune responses when compared with CD45.1→CD45.2 control chimeras.

Z-DTR does not delete monophagocytic lineages or PDCs and immunity was lost in Z-DTR mice, suggesting these subsets are not requisite. To confirm that CD11b^{high} monocytes,

monocyte-derived DCs, and macrophages were not required for immunization, we examined the CD11b-DTR mouse versus wild-type. We observed no significant difference in priming between groups after DT administration, further excluding the contribution of these cells (Fig. 6, D–F) and controlling for the effects of DT administration. These data suggest Zbtb46- and Flt3L-dependent cDCs mediate αCD205gag-p24 priming.

migDCs closely cluster and share expression of immune-dampening genes, and pathways, across species

We were intrigued by the surprising yet consistent observation that deletion of one or multiple subsets of Langerin$^+$ migratory DCs seemed to enhance immunity. Also, collective blockade of skin DC migration enhanced the immune response to priming in vivo; this appeared to occur irrespective of the presence of Flt3L, suggesting migratory DCs might be acting in concert to suppress immunity. We observed close principal component analysis clustering of migDCs to each other when compared with cross-presenting cDCs, monocytes or monocyte-derived DCs, or macrophages (Fig. 7 A). We observed similar clustering of skin-resident DCs in humans when compared with their developmental counter parts in blood (Fig. 7 B). To further investigate this, we sorted three subsets of migDCs and CD8α$^+$ cDCs from the skin-draining LNs from Flt3L-treated mice, seeking transcripts commonly expressed across three migDCs subsets at twofold differential expression when compared with LN-resident CD8α$^+$ DCs. We identified common up-regulation of genes associated with immune suppression across all skin DC subsets when compared with lymphoid-resident cross-presenting DCs mouse (Fig. 7 C). To determine if this occurs in people, we also analyzed transcripts from three subsets of human migDCs isolated from skin versus blood BDCA3$^+$ cross-presenting DCs that were available in the NCBI Gene Expression Omnibus (GEO; see Materials and methods; Haniffa et al., 2012). We observed overlap in the genes expressed in the skin-resident or skin-migrated DCs across both species (Fig. 7 C). We performed our study in Flt3L-treated mice. Prior work has demonstrated immune dampening genes in a murine CD103$^+$ migratory lung DC subset when compared

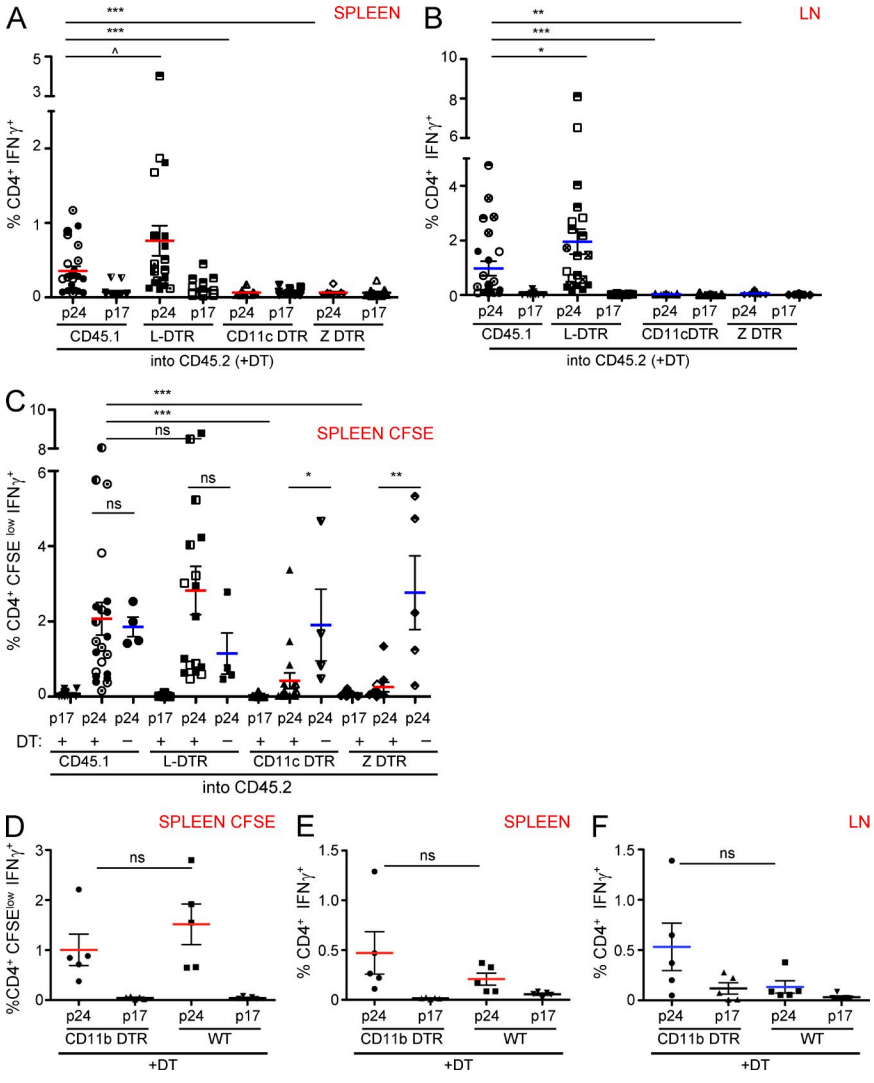

Figure 6. ZBTB46-dependent classical DCs are required for s.c. protein immunization. (A–C) CD45.2 mice were irradiated and reconstituted with bone marrow as indicated. Chimeras received DT on day −3 and −1 to prime and boost immunization with 0.5 µg αCD205 gag-p24. Intracellular cytokine staining immediately ex vivo for (A) Spleen and (B) LN. Black shows staining for p17 peptide control (plus DT) versus red or blue (plus DT) p24 peptide challenge. (C) CFSE dilution of splenocytes after 4 d in culture. (A–C) Pooled from 4–5 independent experiments (n = 3–5 mice per group, based on survival after DT administration). No DT controls (blue) performed once across all 4 groups (n = 4–5 mice per group). Error bars show mean ± SEM. ^, P ≤ 0.1; *, P ≤ 0.05; **, P ≤ 0.01; ***, P ≤ 0.001). (D–F) CD11b DTR versus B6 control mice were administered DT on day −3 and −1 to prime-boost immunization with 0.5 µg αCD205 gag-p24. CFSE dilution of splenocytes after 4 d in culture (D) and intracellular cytokine stainings (E–F). Black shows staining for p17 peptide control (plus DT), red or blue (plus DT) show p24 challenge in wild-type and controls. One representative experiment of n = 4–5 mice per group. Error bars show mean ± SEM. *, P ≤ 0.05; **, P ≤ 0.01; ***, P ≤ 0.001.

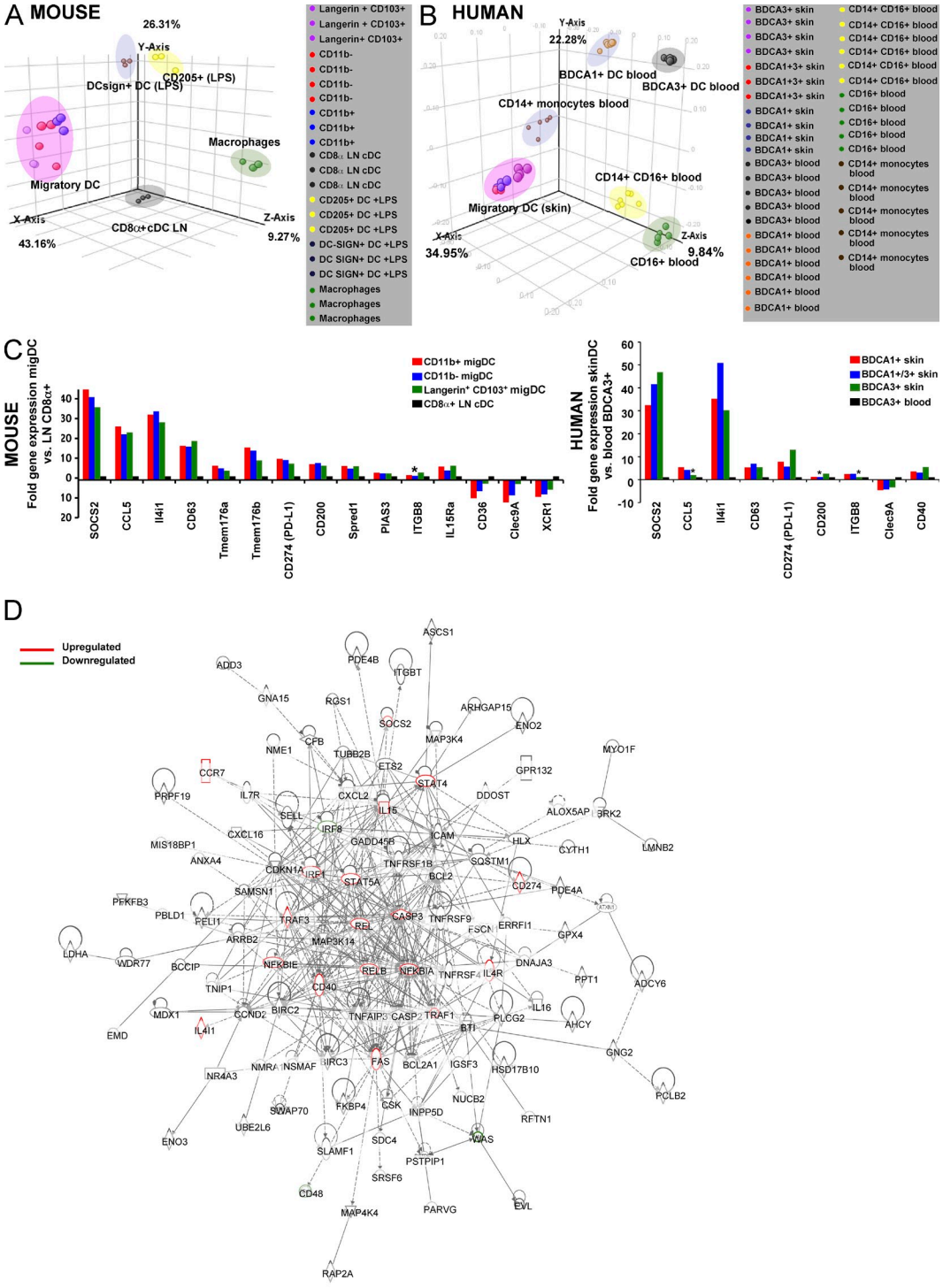

Figure 7. Migratory DC subsets cluster together and share higher expression of immune dampening genes and down-regulation of genes associated with DC activation when compared with cross-presenting DCs in mouse and human. (A) PCA on twofold change (relative to LN CD8α$^+$ cDCs) or greater in the top 15% of all genes (n = 1,290) genes for 3 individual migratory DC, versus LPS-treated CD205$^+$ cDCs, DC-SIGN$^+$ monocyte-derived DCs, and macrophages (mouse); n = 3 or 4 independent sorting experiments and sample replicates. (B) PCA on twofold change (relative to BDCA3$^+$ or BDCA1$^+$ blood DCs) or greater in the top 15% of all genes (n = 920) for human skin-resident versus blood DC and monocyte subsets. (C) Genes shared across all three migDCs subsets with twofold or greater difference compared with CD8α cDCs (mouse) or blood BDCA3$^+$ DC humans: (left) mouse and (right) human skin DC subsets. * denotes the fold difference was under the threshold cut off of twofold in at least one of three migDC subsets. (D) Cross-species IPA. 227 genes commonly up-regulated by twofold or greater across all 3 migratory skin DC subsets compared with classical cross-presenting DCs in both mouse and human. Red represents up-regulated pathways; green represents down-regulated pathways.

with CD8α+ lung LN DCs (Miller et al., 2012). For additional validation, we compared our dataset (Illumina) to additional datasets from skin DC subsets and LN CD8α+ cDCs available in the GEO (see Materials and methods), which were performed by an independent consortium on a different array platform (Affymetrix) and in the absence of Flt3L treatment (Fig. S3). We observed the same trend, which was unaltered by Flt3L treatment. Murine transcripts included SOCS2, PIAS3, PD-L1, ITGB8, and Spred1, CD63, IL4i1, IL15Rα, Tmem176A, and Tmem176B. ITGB8 induces the immunosuppressive cytokine TGFβ (Travis et al., 2007). Knockdown of the tetraspanin CD63 in APC enhances T cell function (Petersen et al., 2011). Tmem176A and 176B binding partners inhibit DC maturation (Louvet et al., 2005; Condamine et al., 2010). The immature state of DCs is associated with silencing of antigen specific T cell responses, induction of T regulatory cells, and tolerance to self (Steinman et al., 2003; Ohnmacht et al., 2009). CCL5 is involved in DC migration (Sallusto et al., 2000), dampens airway hyperresponsiveness, and is essential for suppressor functions of T reg cells (Chang et al., 2012). MigDCs also commonly shared reduced expression of gene products and pathways associated with DC activation, function, and regulation, including Clec9A, XCR1, and CD36. Diminished expression of Clec9A may prevent T cell activation (Zhang et al., 2012). The lymphotactin receptor XCR1 is found on CD8α+ cross-presenting DCs. The XCL1–XCR1 axis controls CD8+ T cell cytotoxicity against antigen (Dorner et al., 2009). CD36 down-regulation may alter DC maturation as binding of erythrocytes infected with malaria to DCs via CD36 significantly inhibits DC maturation (Urban et al., 1999), and antibodies against CD36 modulate DC function (Urban et al., 2001) resulting in failure to prime T cells.

To hone in on commonly regulated pathways across species, we performed Ingenuity Pathway Analysis (IPA) of genes shared in the migratory DCs of mouse and humans (Fig. 7 D). SOCS2, IL-15, and PD-L1 and FAS pathways were observed as central to differential migDC gene expression (Fig. 7 D). SOCS2 may act on DCs directly to block activation through STAT3 and NF-κB signaling (Posselt et al., 2011). In human DCs, SOCS2 acts as a negative regulator of DC activity that is normally expressed after TLR-induced DC activation to counter-regulate DCs (Posselt et al., 2011). IL4i1 has a role in antigen processing and presentation (Boulland et al., 2007) and inhibits T cell proliferation (Lasoudris et al., 2011). PD-L1 directly inhibits T cell function (Butte et al., 2007; Zhang et al., 2012). Convergence on IL-15 signaling may suggest skin DC–mediated control of NK cell function (Castillo et al., 2009).

DISCUSSION

s.c. immunization is one of the most potent and common forms of immunization. Nevertheless, it remains incompletely understood in vivo, limiting the design and development of clinical agents to enhance immunity. To elucidate the role of different DC subsets in immune priming, we simultaneously examined development, antigen capture, gene expression profiling, and functional analysis of different DC subsets. We identified Flt3, ZBT46-dependent classical DCs as central to T cell priming to HIV gag-p24. Strikingly, despite enhanced antigen capture and Flt3L dependence, migDCs, including Langerin+CD103+ DCs, dampen the immune response in vivo and share common gene signatures related to blockade of DC and T cell activation. Our data reveal Flt3 signaling is central to productive immunity via classical DCs and suggest Flt3L may have therapeutic potential when coupled to DC-targeted and soluble protein vaccines, as Flt3L enhanced immunity in multiple settings.

During immunization, changes in the distribution and composition of DCs occur. LN-resident and migDCs redistribute their numbers in the skin-draining LN, a change largely accounted for by an increase in the population of Langerin− dermal DCs (Kastenmüller et al., 2011). Although tightly regulated in the steady state (Shadle et al., 1989; Langley et al., 1993), we detect Flt3L immediately after s.c. delivery of protein immunization and note Flt3L administration alters the composition of cDCs and migDCs in the skin-draining LNs. Flt3 receptor signaling is also necessary for productive immunity. Our data therefore suggest Flt3–Flt3L interactions are likely central to changes in the composition of the LN DC compartment after immunization and requisite for immunity. As previously observed in spleen (Bozzacco et al., 2010; Sathe et al., 2011), we note that Flt3L expands PDCs and cDCs in skin-draining LN, with bias to CD8α CD205+ cross-presenting cDCs (Fig. 3, A and B). Flt3L bias to LN-resident cross-presenting DCs and improved antigen capture by DCs are mechanisms that may support enhanced protein immunization. Indeed, newly formed CD24+ Flt3L-dependent precursors to CD8α+ spleen DCs induce stronger viral recall than CD8α+ DCs (Bedoui et al., 2009b). cDCs from Flt3L-treated mice demonstrate a higher percentage of in vitro antigen capture due to a higher fraction of CD8+ CD205+ DCs being represented (Fig. 3, B and C). This does not exclude the possibility Flt3L could alter lymphatic antigen delivery, but suggests differences in composition may be responsible for the observed effect in vivo.

Robust mucosal immunity is of particular importance to preventing the pathogenesis of certain lentiviral infections, such as HIV. Preferential depletion of CD4+ T cells has been noted in the intestinal lamina propria during acute HIV infection (Brenchley and Douek, 2008). Flt3L enhances both CD4+ and CD8+ mucosal immunity in peripheral sites, including lung parenchyma, small intestinal lamina propria, and skin (unpublished data). Enhanced immunity was versatile and occurred with different antigens, microbial mimics, soluble and DC-targeted protein immunization, and increased serum IgG, lymphoid, and mucosal T cell responses. Coupling Flt3L to both soluble and DC-targeted protein vaccines with appropriate adjuvant for cross-presenting cDCs will likely be of clinical benefit.

Given a requirement for FLK and Zbtb46 with exclusion of migDCs, pDCs, monocytes, and macrophages, we demonstrate that Flt3L- ZBTB46-dependent cDCs are central to s.c. priming. T cell priming via LN-resident CD24+ CD8α DCs is consistent with our observation that Flt3L improved

immunization with either TLR 3/MDA5 (polyIC[LC]) and TLR 4 (GLA-SE) microbial mimics as adjuvant. Flt3L-dependent $CD24^{hi}$ DCs from the spleen and BM cultures express higher transcripts for TLR3 and some TLR4, whereas the $CD11b^+$ subset expresses predominantly TLR4 and no TLR3 (Naik et al., 2005). The requirement for cDCs and not migDCs is not likely caused by TLR restriction because $CD103^+$ dermal DCs express higher levels of TLR3 (Jelinek et al., 2011) but are dispensable for immunization with polyIC(LC). Finally, our observations in $CCR7^{-/-}$ mice, also may suggest monocyte-derived DCs are not required in the LN during priming because they require CCR7 for LN entry (Cheong et al., 2010). Although GLA-SE is a microbial mimic of LPS, and LPS induces monocyte-derived DCs, we observe that GLA-SE may act as adjuvant independently of monocyte-derived DCs in the skin-draining LNs. This was further validated using CD11b DTR mice in which deletion of monocytes and monocyte-derived DCs, but not $CD8\alpha^+$ $CD205^+$ cDCs, occurs (Choi et al., 2011), which did not impair $CD4^+$ IFN-γ responses.

Our data support a functional and genetically programmed role for migDCs in dampening immunity. Current vaccine design efforts are centered on targeting antigen to skin DCs and may inadvertently trigger a program of immune suppression. At high and limiting dose αCD205-gag p24, we do not observe a requirement $Langerin^+$ DCs in s.c. immunization. Rather we observe enhanced T and B cell immunity. Enhanced immunity to s.c. and i.d. antigen are observed in the complete absence of skin DC migration to the draining LNs. Consistent with a role in dampening immunity in vivo, three individual skin DC subsets share common expression of genes associated with tolerance when compared with lymphoid and blood cross-presenting DCs. These included common programs shared across species that block DC migration and activation, and those involved in direct inhibition of T cell activation, such as PD-L1. Thus, the immune response likely results from a complex interplay of tolerizing and immunizing DC activity in LNs. The cues that dictate when migDCs are poised to induce tolerance versus immunity to self and nonself-antigens remain to be further investigated. These cues may be conferred by the cutaneous or peripheral microenvironment and likely extend beyond hematopoietic lineage specification. Our study suggests $Langerin^+CD103^+$ DCs from tissue directly oppose the activity $CD8\alpha$ cDCs in LNs in vivo despite common origin, shared developmental pathways, and irrespective of developmental potentiation with Flt3L. Indeed, we find migDCs from both Flt3L-treated and untreated mice share elevated expression of immune-dampening gene signatures and pathways (Fig. 7 and Fig. S3).

In contrast to a deterministic model in which distinct populations of DCs are developmentally programmed, the role of different DC subsets in priming and tolerance could relate to their spatial and temporal distribution in the LN, tissue residence, and antigen access. cDCs lie close to the LN reticular system, or conduits, where they rapidly uptake and present soluble antigen from lymph (Sixt et al., 2005). migDC subsets carry high concentrations of processed antigens to the LN inner and outer paracortex near HEVs (Bajénoff et al., 2003; Kissenpfennig et al., 2005) and arrive in the LN later after immunization (Itano et al., 2003). That we observe enhanced antigen capture by migDCs in LNs is consistent with prior observations of soluble antigen pE–I–Ab complexes detected on skin-derived DCs already present in the LNs as early as 30 min after s.c. antigen injection (Itano et al., 2003). Based on the early kinetics of peptide complex detection, migDCs in LN were thought to initiate T cell priming. However, when the injection site is removed 5 h after s.c. priming, preventing the arrival of additional migDCs from periphery to LN, clonal proliferation is not impaired, suggesting redundancy of migDCs that acquired antigens in the periphery and traffic into the LN. However, injection site removal studies cannot exclude the contribution of preexisting LN-resident migDCs (Itano et al., 2003). Rather, when we tested $CCR7^{-/-}$ mice where migDCs are entirely absent from the LN at the time of priming, we observe enhanced not diminished in vivo immune priming supporting a role for migDCs at the LN in dampening immunity and further supported by their common transcriptomics program.

Previous studies addressing DC subset contributions have largely examined the $CD4^+$ T cells response to s.c. OVA immunization (Allenspach et al., 2008). In this system, immune responses depended on radio-resistant skin DCs (i.e., mainly LCs) in the draining LNs. Differences in our observations from such work may result from several notable differences in the model systems used, including the antigen (HIV gag-p24 vs. OVA), the adjuvant (microbial mimic vs. complete or incomplete freund's adjuvant), deliver strategy (DC-targeted vs. nontargeted), differences in the naive polyclonal repertoire in our study versus intravenous adoptive transfer of a single-affinity clone (OT-II), and the model system used to test the contribution of migDCs (restricted migration and complete absence in the LN in $CCR7^{-/-}$ or DTR depletion [our study] versus normal migration capacity of migDCs but with impaired MHCII presentation [Allenspach et al., 2008]). Additional work using OT-II T cell transfer and immunization with chemically coupled αCD205-OVA in the $CCR7^{-/-}$ versus control mice observed a diminished T cell response in $CCR7^{-/-}$ mice (Ohl et al., 2004). Therefore, the difference we observe compared with previous studies with OVA and OT-II is most likely related to the nature of the antigen and uniform T cell repertoire in the setting of transgenic models rather than antigen delivery (DC targeting), adjuvant, and the model system used to distinguish migDCs from LN-resident DCs. Indeed, in prior experiments when the concentration of OVA was increased the requirement for migDCs was relieved (Allenspach et al., 2008). Thus, dependence for the migDCs in the OVA transgenic system may relate to specifics of that system, such as affinity of the clone, low-dose antigen, the number of peptide MHCII complexes, the distribution of intravenously transferred transgenic T cells, and competition of naive transgenic cells for antigen. Consistently, migDCs failed to induce delayed proliferation of OT-II cells in the absence

of lymphoid-resident DC antigen presentation (Allenspach et al., 2008), supporting our observation LN-resident DCs are required to initiate immunity and that lymphoid-resident DCs selectively trap antigen-specific lymphocytes in the draining LN (Itano et al., 2003). Our initial observation that migratory DCs dampen the immune response to high- and low-dose antigen was validated with four selective DC ablation models and transcriptome analyses.

Lastly, we note that CCR7 is dispensable on both T cells and DCs for productive immunity. Though migDCs are entirely CCR7-dependent, naive T cell entry into LN is partially dependent on CCR7 and reduced to 30–50% of wild-type levels in peripheral LNs (Förster et al., 1999). T cells can be classified as naive central memory (T_{CM}) CD45RA$^-$ CCR7$^+$, effector memory (T_{EM}) CD45RA$^-$ CCR7$^-$ or terminally differentiated effector cells (T_{EMRA}) CD45RA$^+$ CCR7$^-$ (Sallusto et al., 1999; Sallusto and Lanzavecchia, 2009; Pepper et al., 2010). That CCR7 dependence was not observed on T cells may relate to the observation in vaccinia virus and yellow fever vaccines that memory T cells within 2 wk of priming are predominantly CCR7$^-$ and exhibit strong proliferation in vitro, suggesting a lack of terminal differentiation (Ahmed and Akondy, 2011).

Advances in immunotherapy to block immunosuppression include CTLA-4 and PD-L1 blockade, and dramatically expand the therapeutic window for immune priming. Protein immunization offers a safe and efficacious strategy. We demonstrate the Flt3 pathway is central to protein immunization and can be exploited to potentiate immunity via cDCs. Our data further reveal that a robust T cell and humoral immunity to protein immunization with clinically relevant vaccines, and with a polyclonal T cell repertoire, is centered on ZBTB46- and Flt3L-dependent cDCs. We establish skin-derived migDCs, including Langerin$^+$ 103$^+$ DCs, are not required at the LN for s.c. protein vaccination immunization. Instead these populations collectively and individually dampen immunity and share common expression of genes associated with immune inhibition. Though Langerin$^+$CD103$^+$ DCs of the skin share developmental origin with CD8α cDCs in lymphoid tissue, they may be conditioned by tissue microenvironment to inhibit DC and T cell activation. This cannot be overcome by enhancing their numbers, antigen capture, or developmental conditioning. Thus, future immunization strategies for the clinic will couple likely protein immunization and Flt3L treatment to target antigen to, and simultaneously potentiate the development of and antigen capture by, LN-resident cDCs.

MATERIALS AND METHODS

Mice, chimerization, and deletion. C57BL/6 mice (B6) were purchased from Taconic Labs or bred at The Rockefeller University. The Langerin-DTR mouse was developed to distinguish between the functional attributes of Langerin$^+$ and other DC subsets (Bennett et al., 2005). 0.5–1 µg DT (Sigma-Aldrich) was administered per average 25–30 g mouse as described for all DTR-based transgenic strains used, including the CD11b and CD11c DTR (Zaft et al., 2005) that were purchased from The Jackson Laboratory. CCR7$^{-/-}$ mice were bred at The Rockefeller University after purchase from The Jackson Laboratory and are described with respect to defects in the skin-derived DC migration (Martín-Fontecha et al., 2003, 2008). Langerin-GFP mice were generously provided by B. Malissen, bred as homozygotes at The Rockefeller University, and have been previously described (Kissenpfennig et al., 2005). BM chimeras used 8–9-wk-old irradiated recipients (500 cGy plus 550 cGy) with 3 h between irradiations; cell suspensions of BM were injected intravenously immediately after (3×10^6 BM cells transferred per recipient). Mice were maintained after radiation on antibiotic supplemented food (TestDiet) for 12 wk before use. All mice were housed in specific pathogen–free conditions. Protocols were approved by the Rockefeller University Animal Care and Use Committee.

Tissue harvest and cell preparation of DC. 6–8-wk-old C57BL/6 F or Langerin-GFP mice were injected s.c. to the flank with endotoxin-free (<0.0064 EU/mg), GMP grade, recombinant human Flt3L (Celldex) at 10 µg/mouse/day diluted in sterile PBS for 10–14 d. For sorting skin DC subsets, Flt3L-treated Langerin GFP mice were used to obtain sufficient numbers of migratory DCs from the skin-draining LNs. Skin-draining LN and spleen was isolated from individual mice, teased or ballooned, and incubated for 25 min at 37°C in Collagenase D (400 U/ml, Roche) in Hanks' Balanced Salt Buffer (Invitrogen). After incubation, 0.5 M EDTA was added to a final concentration of 10 mM EDTA for disruption of DC–T cell complexes and the sample was incubated for an additional 5 min at 37°C. For spleen cell preparation, ACK lysis of red cells was performed. Undigested fibrous material was filtered through a 70-µm cell strainer. Subsequent washed were performed with ice-cold PBS with 2% FCS. For crawl-out assay, individual ears were harvested, washed in 70% EtOH and split dermal side down into complete-RPMI media. At 72 h, cell suspensions were isolated and filtered. The pellet was washed twice and incubated in Fc block with 2% rat serum before cell surface marker antibody staining.

After size, live/dead, and exclusion criteria (CD3, CD19, NK1.1 exclusion), DC subsets were sorted as described (Fig. 3 and Fig. S2). RNA was prepared by standard methods using TRIzol (Invitrogen) and further purified using RNeasy MinElute clean up (QIAGEN). Purity analysis was done by nanodrop and Eukaryote Total RNA Pico Series II (Agilent). RNA was amplified and hybridized on the Illumina MouseRef-8 v2.0 Expression BeadChip.

Vaccination protocol. Age, gender-matched control, and experimental mice were injected daily during both the prime and boost phase by i.p. injection with Flt3L, as above, in sterile PBS, or by PBS alone (control) for 10 d. At day 8, αCD205-gag p24 or αCD205-OVA was injected s.c. into the footpad or by the i.p. route, as indicated with 20 µg of GLA-SE (Immune Design) or 25 µg of polyIC stabilized with poly-L-lysine (poly IC[LC]; Longhi et al., 2009).

Boost vaccination was administered exactly 4 wk later. For s.c. priming to αCD205-gag p24, mice in all groups were sacrificed 7 d after immunization. For s.c. priming to αCD205-OVA, mice were sacrificed at day 11after boost for IP priming at 21 d. In mice vaccinated to αCD205-gag p24, peptide challenge with p24 pools or p17 (control) pools at 1 µg/ml for intracellular cytokine staining with 2 µg/ml anti-CD28 antibody was added, and at 0.05 µg/ml for CFSE 4 d cultures. For mice vaccinated to αCD205-OVA, OT-I and OT-II peptides were pooled versus p24 (control) at 1 µg/ml for ICS with 2 µg/ml anti-CD28 antibody, and for CFSE cultures at 0.05 µg/ml.

T cell isolation for proliferation assay or intracellular cytokine stain (spleen, lungs, and LN). Individual vaccinated mice were sacrificed, and serum collected by cardiac bleed with separation of serum from heme by centrifugation at 13,000 rpm in BD microtainer serum separator tubes (ref. 365956) in a table-top rotor (Eppendorf 5417R) at 4°C. Intracardiac perfusion was performed with PBS into the right ventricle to balloon the lungs and flush leukocytes and RBCs from the pulmonary circulation. Individual lung lobes were dissected, taking care to avoid the mediastinal LN, ballooned with Collagenase D, and then further dissociated with pressure using the end of a 5-ml syringe, followed by incubation at 37°C for 20 min. 10 mM EDTA was added for the last 5 min of incubation. ACK lysis was performed as above. Spleens and LN were harvested in RPMI complete media with 5% FCS, mashed between 2 sterile glass slides, washed with RPMI complete media, and then filtered through a 70-µM filter. Spleen samples but not LNs went

through subsequent ACK lysis as described, and were washed twice and counted. As described by Trumpfheller et al. (2008) 500K splenocytes were incubated for 6 h at 37°C with p24 pooled peptides or p17 pooled peptides at a final concentration of 1 μg/ml with 2 μg/ml anti-CD28 antibody (clone 37.51; American Type Culture Collection). After 1-h incubation, Brefeldin A was added to a final concentration of 10 μg/ml for the remaining 5 h to allow intracellular cytokine accumulation. For all subsequent steps, cells were washed and stained in ice-cold PBS with 2% FCS. For proliferation assays, splenocytes were labeled with 1 μM/ml CFSE (Sigma-Aldrich) and plated with 0.05 μg/ml p24 or p17 peptide pool. At 72 h, supernatants were harvested for cytokine ELISA. At 96 h, cells were isolated, washed, and intracellular cytokine staining was performed as previously described.

Serum gag-specific IgG and Flt3L ELISA. Serum was prepared by cardiac bleed, followed by serum separation using microtainer tubes (365956; BD). Serum gag-specific ELISA was performed by coating NUNC plates (Apogent 80040 LE 0903) with 2 μg/ml of gag p24 recombinant protein in PBS or ELISA coating buffer overnight at 4°C. Plates were washed 3–5 times with PBS and blocked with Blocking solution (1× PBS, 5% goat serum, and 0.1% Tween-20) for 1 h at 37°C, followed by sample addition at serial 10-fold titration (dilutions made into blocking solution) for 2 h at 25°C, followed by 3–5 subsequent washes. A 1:10,000 dilution of goat anti–mouse IgG HRP (Jackson ImmunoResearch Laboratories; 115–035-071) was added according to standard protocols for 1 h at 37°C, the plate was washed 3–5 times before addition of 100 μl 1X TMB Substrate Solution (eBioscience; 00–4201-56), stopped with addition of 2N sulfuric acid, and read at 450/470 nm. Murine Flt3L ELISA was performed on serum isolated from 3–5 individual mice using the RD mFlt3L ELISA kit (E90038Mu).

Lamina propria isolation. To prepare single intestinal cell suspension, part of small bowel including jejunum and ileum or a large bowel (cecum and colon) were excised. Peyer's patches were removed from the small intestinal tissue. Intestinal lumen was exposed by a longitudinal incision and the tissue was cut to a pasty consistency. Next, intestinal tissues were incubated in RPMI with 1.3 mM EDTA (CellGro) on a 37°C shaker for 1 h. The supernatants containing intestinal epithelial cell (IEC) with some superficial villous cells, were discarded. Tissue was washed thrice with RPMI to remove EDTA. Tissue was digested with 0.2 mg/ml of type IV collagenase (Sigma-Aldrich) at 37°C for 1 h. Tissue was then homogenized, filtered, and washed. The resulting cell suspension was layered on a 44%/66% Percoll (GE Healthcare) gradient and the interface was collected to obtain an enriched mononuclear cell population. Cell were washed and resuspended in complete medium at a density of 2–5 × 10^6 cells/ml. Recall responses were examined as described above.

Antibodies, live/dead dye, CFSE, FITC painting, and staining reagents. The following reagents were obtained from BD, eBioscience, or BioLegend: anti-Langerin (eBioL31), anti-CD11c (N418), anti–IFN-γ (XMG1.2), anti-CD4 (RM4-5), anti-CD8α (53–6.7), anti-CD11b (M1/70), anti-CD103 (2 E7), anti–Armenian Hamster IgG Isotype Control (eBio299Arm), anti–rat IgG2a Isotype Control (eBR2a), anti-CD3 (500A2), anti-CD45 (30-F11), anti-CD205 (NLDC-145), anti-EPCAM (G8.8), anti-CD24 (M1/69), anti-F4/80 (BM8), anti-CD115 (AFS98), anti-PDCA1 (ebio927), anti-Ly6c (HK1.4), anti-B220 (RA3-6B2), anti–I-A/I-E (M5/114.15.2), anti-CD3 (17A2), anti-CD19 (eBio1D3), and anti-NK1.1 (PK136). AQUA (L34957) was from Invitrogen. Cytofix/Cytoperm kit was from BD. CFSE was obtained from Sigma-Aldrich. Anti-CD205 (NLDC-145) was produced in the Steinman laboratory and conjugated to Alexa Fluor 488 or 647. Other reagents included PBS and FBS (Invitrogen), ACK lysing buffer (BioSource). Staining with Langerin and in some experiments for CD205 was performed with cell surface and intracellular label. IFN-γ staining was performed after cell surface label of T cell markers by intracellular cytokine staining using Fix/Perm and Perm/Wash buffers (BD). Langerin staining was performed by intracellular stain with anti-Langerin (L31) as previously described (Cheong et al., 2007). For intracellular blocking, 2% rat serum was diluted into perm/wash buffer. All extracellular staining was performed in ice cold PBS with 2% FCS. FITC painting was performed on the flank with 1:1 1% FITC in acetone/dibutyl phthalate for 18–24 h before harvest.

Flow cytometry and gating. Cells were stained on ice in PBS with 2.0% (vol/vol) FCS. LSR II (BD) was used for multiparameter flow cytometry of stained cell suspensions, followed by analysis with FlowJo software (Tree Star). For vaccine analysis T cells from individual organs were gated by scatter, singlets, exclusion of dead cells, $CD3^+$, $CD4^+$ versus $CD8^+$ IFN-γ and in proliferative assays by CFSE low, IFN-γ^+ cells (Fig. S1, sample gating). For LN DC subsets, sample gating is depicted (Fig. S2 A).

Microarray analysis, normalization and data analysis. Microarray data is available macrophages, monocyte-derived LN DCs, LPS-treated classical DCs in LNs, and LNs of Flt3L-treated mice from GEO under accession no. GSE53588. Additional murine microarray files (Miller et al., 2012) were downloaded from GEO under the accession no. GSE15907 (subset data from accession nos. GSM538255–GSM538257 and GSM538268–GSM538279). A custom chip technology for Affymetrix Mouse Gene 1.0 ST was created to import the raw data into GeneSpring NGS. Human microarray files (Haniffa et al., 2012) were downloaded from NCBI Gene Expression Omnibus under the accession no. GSE35459 (subset data from accession nos. GSM868894–GSM868898, GSM868910–GSM868917, and GSM868922–GSM868925). A custom chip technology for Illumina HumanHT-12V4.0 expression BeadChip was created to import the raw data into GeneSpring NGS.

Raw files were preprocessed and normalized using GeneSpring GX Version 12.5 RMA algorithm. Resultant data were pooled into groups by various subtypes. The results of replicates were averaged. Normalized data were filtered for gene encoding regulators with a coefficient of variation of less than 0.5 in population replicates. Individual dermal migratory DCs in LNs were compared against LN-resident $CD8\alpha^+$ DCs, and differentially expressed genes of twofolds or more were assessed by variance across the DC populations with the one-way (ANOVA), corrected for multiple hypotheses testing with Benjamini and Hochberg FDR of <0.05.

Statistical analysis. For data reported in vaccine experiments, error bars represent the standard error of the mean plotted between 3–5 individual animals per experiment per replicate. Statistical analysis for ICS and CFSE was performed using the Mann-Whitney test between two groups was done using Prism software ($P > 0.05$, not significant [ns], *, $P \leq 0.05$; **, $P \leq 0.01$; ***, $P \leq 0.001$). For serum Flt3L ELISA detection (Mann-Whitney test) and DC expansion (unpaired Student's *t* test), error bars represent the SD between three to five individual mice per group. For serum gag-p24 or OVA IgG detection, error bars represent the mean ± SEM and were analyzed using an unpaired Student's *t* test.

Online supplemental material. Fig. S1 shows the gating schema for intracellular cytokine staining assays. Fig. S2 shows the gating of LN-resident DC subsets. Fig. S3 depicts fold change in individual migratory skin DC subsets from our Flt3L-treated mice on the Illumina platform, versus Imgen consortium data on untreated mice on the Affymetrix platform. Online supplemental material is available at http://www.jem.org/cgi/content/full/jem.20131397/DC1.

We are deeply grateful to Ralph M. Steinman for his mentorship, support, and wisdom. The authors thank Christine Trumpfheller for advice with αCD205-HIV gag immunization, Tibor Keler and Celldex therapeutics for use of recombinant Flt3L, Immune Design Corporation for use of GLA, Judy Adams for assistance with preparation of the figures, Jennifer Oghene, Anthony Rodriguez, and Sandy King for technical assistance, and Marguerite Nulty for administrative assistance. We thank Michelle Lowes and Andrew Sikora for critical reading of the manuscript.

N. Anandasabapathy was supported in part by grant no. RR024142 from the National Center for Research Resources, National Institutes of Health (NIH), the Dermatology Foundation, and supported by NIH grants AI40045, 81677, and 13013 (to R.M. Steinman)and National Institute of Arthritis and Musculoskeletal and Skin Diseases AR063461-01A1 and Klarman family foundation grants (to

N. Anandasabapathy). B.E. Clausen is a VIDI fellow of The Netherlands Organization for Scientific Research. C. Cheong was supported by the New York Community Trust Frances Florio Fund.

Ralph Steinman and Michel Nussenzweig served/serve on the scientific advisory board and held/hold stock options in Celldex Therapeutics. The authors have no additional conflicting financial interests.

Submitted: 3 July 2013
Accepted: 18 July 2014

REFERENCES

Ahmed, R., and R.S. Akondy. 2011. Insights into human CD8(+) T-cell memory using the yellow fever and smallpox vaccines. *Immunol. Cell Biol.* 89:340–345. http://dx.doi.org/10.1038/icb.2010.155

Allenspach, E.J., M.P. Lemos, P.M. Porrett, L.A. Turka, and T.M. Laufer. 2008. Migratory and lymphoid-resident dendritic cells cooperate to efficiently prime naive CD4 T cells. *Immunity*. 29:795–806. http://dx.doi.org/10.1016/j.immuni.2008.08.013

Bajénoff, M., S. Granjeaud, and S. Guerder. 2003. The strategy of T cell antigen-presenting cell encounter in antigen-draining lymph nodes revealed by imaging of initial T cell activation. *J. Exp. Med.* 198:715–724. http://dx.doi.org/10.1084/jem.20030167

Bedoui, S., S. Prato, J. Mintern, T. Gebhardt, Y. Zhan, A.M. Lew, W.R. Heath, J.A. Villadangos, and E. Segura. 2009a. Characterization of an immediate splenic precursor of CD8+ dendritic cells capable of inducing antiviral T cell responses. *J. Immunol.* 182:4200–4207. http://dx.doi.org/10.4049/jimmunol.0802286

Bedoui, S., P.G. Whitney, J. Waithman, L. Eidsmo, L. Wakim, I. Caminschi, R.S. Allan, M. Wojtasiak, K. Shortman, F.R. Carbone, et al. 2009b. Cross-presentation of viral and self antigens by skin-derived CD103+ dendritic cells. *Nat. Immunol.* 10:488–495. http://dx.doi.org/10.1038/ni.1724

Bennett, C.L., E. van Rijn, S. Jung, K. Inaba, R.M. Steinman, M.L. Kapsenberg, and B.E. Clausen. 2005. Inducible ablation of mouse Langerhans cells diminishes but fails to abrogate contact hypersensitivity. *J. Cell Biol.* 169:569–576. http://dx.doi.org/10.1083/jcb.200501071

Boulland, M.L., J. Marquet, V. Molinier-Frenkel, P. Möller, C. Guiter, F. Lasoudris, C. Copie-Bergman, M. Baia, P. Gaulard, K. Leroy, and F. Castellano. 2007. Human IL4I1 is a secreted L-phenylalanine oxidase expressed by mature dendritic cells that inhibits T-lymphocyte proliferation. *Blood*. 110:220–227. http://dx.doi.org/10.1182/blood-2006-07-036210

Bozzacco, L., C. Trumpfheller, Y. Huang, M.P. Longhi, I. Shimeliovich, J.D. Schauer, C.G. Park, and R.M. Steinman. 2010. HIV gag protein is efficiently cross-presented when targeted with an antibody towards the DEC-205 receptor in Flt3 ligand-mobilized murine DC. *Eur. J. Immunol.* 40:36–46. http://dx.doi.org/10.1002/eji.200939748

Brasel, K., H.J. McKenna, P.J. Morrissey, K. Charrier, A.E. Morris, C.C. Lee, D.E. Williams, and S.D. Lyman. 1996. Hematologic effects of flt3 ligand in vivo in mice. *Blood*. 88:2004–2012.

Brenchley, J.M., and D.C. Douek. 2008. HIV infection and the gastrointestinal immune system. *Mucosal Immunol.* 1:23–30. http://dx.doi.org/10.1038/mi.2007.1

Butte, M.J., M.E. Keir, T.B. Phamduy, A.H. Sharpe, and G.J. Freeman. 2007. Programmed death-1 ligand 1 interacts specifically with the B7-1 costimulatory molecule to inhibit T cell responses. *Immunity*. 27:111–122. http://dx.doi.org/10.1016/j.immuni.2007.05.016

Castillo, E.F., S.W. Stonier, L. Frasca, and K.S. Schluns. 2009. Dendritic cells support the in vivo development and maintenance of NK cells via IL-15 trans-presentation. *J. Immunol.* 183:4948–4956. http://dx.doi.org/10.4049/jimmunol.0900719

Chang, L.Y., Y.C. Lin, C.W. Kang, C.Y. Hsu, Y.Y. Chu, C.T. Huang, Y.J. Day, T.C. Chen, C.T. Yeh, and C.Y. Lin. 2012. The indispensable role of CCR5 for in vivo suppressor function of tumor-derived CD103+ effector/memory regulatory T cells. *J. Immunol.* 189:567–574. http://dx.doi.org/10.4049/jimmunol.1200266

Cheong, C., J. Idoyaga, Y. Do, M. Pack, S.H. Park, H. Lee, Y.S. Kang, J.H. Choi, J.Y. Kim, A. Bonito, et al. 2007. Production of monoclonal antibodies that recognize the extracellular domain of mouse langerin/CD207. *J. Immunol. Methods*. 324:48–62. http://dx.doi.org/10.1016/j.jim.2007.05.001

Cheong, C., I. Matos, J.H. Choi, D.B. Dandamudi, E. Shrestha, M.P. Longhi, K.L. Jeffrey, R.M. Anthony, C. Kluger, G. Nchinda, et al. 2010. Microbial stimulation fully differentiates monocytes to DC-SIGN/CD209(+) dendritic cells for immune T cell areas. *Cell*. 143:416–429. http://dx.doi.org/10.1016/j.cell.2010.09.039

Choi, J.H., C. Cheong, D.B. Dandamudi, C.G. Park, A. Rodriguez, S. Mehandru, K. Velinzon, I.H. Jung, J.Y. Yoo, G.T. Oh, and R.M. Steinman. 2011. Flt3 signaling-dependent dendritic cells protect against atherosclerosis. *Immunity*. 35:819–831.

Condamine, T., L. Le Texier, D. Howie, A. Lavault, M. Hill, F. Halary, S. Cobbold, H. Waldmann, M.C. Cuturi, and E. Chiffoleau. 2010. Tmem176B and Tmem176A are associated with the immature state of dendritic cells. *J. Leukoc. Biol.* 88:507–515. http://dx.doi.org/10.1189/jlb.1109738

Dorner, B.G., M.B. Dorner, X. Zhou, C. Opitz, A. Mora, S. Güttler, A. Hutloff, H.W. Mages, K. Ranke, M. Schaefer, et al. 2009. Selective expression of the chemokine receptor XCR1 on cross-presenting dendritic cells determines cooperation with CD8+ T cells. *Immunity*. 31:823–833. http://dx.doi.org/10.1016/j.immuni.2009.08.027

Duthie, M.S., H.P. Windish, C.B. Fox, and S.G. Reed. 2011. Use of defined TLR ligands as adjuvants within human vaccines. *Immunol. Rev.* 239:178–196. http://dx.doi.org/10.1111/j.1600-065X.2010.00978.x

Eidenschenk, C., K. Crozat, P. Krebs, R. Arens, D. Popkin, C.N. Arnold, A.L. Blasius, C.A. Benedict, E.M. Moresco, Y. Xia, and B. Beutler. 2010. Flt3 permits survival during infection by rendering dendritic cells competent to activate NK cells. *Proc. Natl. Acad. Sci. USA*. 107:9759–9764. http://dx.doi.org/10.1073/pnas.1005186107

Förster, R., A. Schubel, D. Breitfeld, E. Kremmer, I. Renner-Müller, E. Wolf, and M. Lipp. 1999. CCR7 coordinates the primary immune response by establishing functional microenvironments in secondary lymphoid organs. *Cell*. 99:23–33. http://dx.doi.org/10.1016/S0092-8674(00)80059-8

Ginhoux, F., K. Liu, J. Helft, M. Bogunovic, M. Greter, D. Hashimoto, J. Price, N. Yin, J. Bromberg, S.A. Lira, et al. 2009. The origin and development of nonlymphoid tissue CD103+ DCs. *J. Exp. Med.* 206:3115–3130. http://dx.doi.org/10.1084/jem.20091756

Gitlin, L., W. Barchet, S. Gilfillan, M. Cella, B. Beutler, R.A. Flavell, M.S. Diamond, and M. Colonna. 2006. Essential role of mda-5 in type I IFN responses to polyriboinosinic:polyribocytidylic acid and encephalomyocarditis picornavirus. *Proc. Natl. Acad. Sci. USA*. 103:8459–8464. http://dx.doi.org/10.1073/pnas.0603082103

Guermonprez, P., J. Helft, C. Claser, S. Deroubaix, H. Karanje, A. Gazumyan, G. Darasse-Jeze, S.B. Telerman, G. Breton, H.A. Schreiber, et al. 2013. Inflammatory Flt3l is essential to mobilize dendritic cells and for T cell responses during *Plasmodium* infection. *Nat. Med.* 19:730–738.

Haniffa, M., A. Shin, V. Bigley, N. McGovern, P. Teo, P. See, P.S. Wasan, X.N. Wang, F. Malinarich, B. Malleret, et al. 2012. Human tissues contain CD141hi cross-presenting dendritic cells with functional homology to mouse CD103+ nonlymphoid dendritic cells. *Immunity*. 37:60–73. http://dx.doi.org/10.1016/j.immuni.2012.04.012

Henri, S., M. Guilliams, L.F. Poulin, S. Tamoutounour, L. Ardouin, M. Dalod, and B. Malissen. 2010a. Disentangling the complexity of the skin dendritic cell network. *Immunol. Cell Biol.* 88:366–375. http://dx.doi.org/10.1038/icb.2010.34

Henri, S., L.F. Poulin, S. Tamoutounour, L. Ardouin, M. Guilliams, B. de Bovis, E. Devilard, C. Viret, H. Azukizawa, A. Kissenpfennig, and B. Malissen. 2010b. CD207+ CD103+ dermal dendritic cells cross-present keratinocyte-derived antigens irrespective of the presence of Langerhans cells. *J. Exp. Med.* 207:189–206. http://dx.doi.org/10.1084/jem.20091964

Itano, A.A., S.J. McSorley, R.L. Reinhardt, B.D. Ehst, E. Ingulli, A.Y. Rudensky, and M.K. Jenkins. 2003. Distinct dendritic cell populations sequentially present antigen to CD4 T cells and stimulate different aspects of cell-mediated immunity. *Immunity*. 19:47–57. http://dx.doi.org/10.1016/S1074-7613(03)00175-4

Jelinek, I., J.N. Leonard, G.E. Price, K.N. Brown, A. Meyer-Manlapat, P.K. Goldsmith, Y. Wang, D. Venzon, S.L. Epstein, and D.M. Segal. 2011. TLR3-specific double-stranded RNA oligonucleotide adjuvants induce dendritic cell cross-presentation, CTL responses, and antiviral protection. *J. Immunol.* 186:2422–2429. http://dx.doi.org/10.4049/jimmunol.1002845

Kastenmüller, K., U. Wille-Reece, R.W. Lindsay, L.R. Trager, P.A. Darrah, B.J. Flynn, M.R. Becker, M.C. Udey, B.E. Clausen, B.Z. Igyarto, et al. 2011. Protective T cell immunity in mice following protein-TLR7/8 agonist-conjugate immunization requires aggregation, type I IFN, and multiple DC subsets. *J. Clin. Invest.* 121:1782–1796. http://dx.doi.org/10.1172/JCI45416

Kissenpfennig, A., S. Henri, B. Dubois, C. Laplace-Builhé, P. Perrin, N. Romani, C.H. Tripp, P. Douillard, L. Leserman, D. Kaiserlian, et al. 2005. Dynamics and function of Langerhans cells in vivo: dermal dendritic cells colonize lymph node areas distinct from slower migrating Langerhans cells. *Immunity*. 22:643–654. http://dx.doi.org/10.1016/j.immuni.2005.04.004

Langley, K.E., L.G. Bennett, J. Wypych, S.A. Yancik, X.D. Liu, K.R. Westcott, D.G. Chang, K.A. Smith, and K.M. Zsebo. 1993. Soluble stem cell factor in human serum. *Blood*. 81:656–660.

Lasoudris, F., C. Cousin, A. Prevost-Blondel, N. Martin-Garcia, I. Abd-Alsamad, N. Ortonne, J.P. Farcet, F. Castellano, and V. Molinier-Frenkel. 2011. IL4I1: an inhibitor of the CD8$^+$ antitumor T-cell response in vivo. *Eur. J. Immunol.* 41:1629–1638. http://dx.doi.org/10.1002/eji.201041119

Liu, K., C. Waskow, X. Liu, K. Yao, J. Hoh, and M. Nussenzweig. 2007. Origin of dendritic cells in peripheral lymphoid organs of mice. *Nat. Immunol.* 8:578–583. http://dx.doi.org/10.1038/ni1462

Liu, K., G.D. Victora, T.A. Schwickert, P. Guermonprez, M.M. Meredith, K. Yao, F.F. Chu, G.J. Randolph, A.Y. Rudensky, and M. Nussenzweig. 2009. In vivo analysis of dendritic cell development and homeostasis. *Science*. 324:392–397.

Longhi, M.P., C. Trumpfheller, J. Idoyaga, M. Caskey, I. Matos, C. Kluger, A.M. Salazar, M. Colonna, and R.M. Steinman. 2009. Dendritic cells require a systemic type I interferon response to mature and induce CD4+ Th1 immunity with poly IC as adjuvant. *J. Exp. Med.* 206:1589–1602. http://dx.doi.org/10.1084/jem.20090247

Louvet, C., E. Chiffoleau, M. Heslan, L. Tesson, J.M. Heslan, R. Brion, G. Bériou, C. Guillonneau, J. Khalife, I. Anegon, and M.C. Cuturi. 2005. Identification of a new member of the CD20/FcepsilonRIbeta family overexpressed in tolerated allografts. *Am. J. Transplant.* 5:2143–2153. http://dx.doi.org/10.1111/j.1600-6143.2005.01007.x

Lyman, S.D., and H.J. McKenna. 2003. Flt3 ligand. *In* The Cytokine Handbook. A. Thomson, editor. Academic Press. pp. 989–1010. http://dx.doi.org/10.1016/B978-012689663-3/50046-6

Maraskovsky, E., K. Brasel, M. Teepe, E.R. Roux, S.D. Lyman, K. Shortman, and H.J. McKenna. 1996. Dramatic increase in the numbers of functionally mature dendritic cells in Flt3 ligand-treated mice: multiple dendritic cell subpopulations identified. *J. Exp. Med.* 184:1953–1962. http://dx.doi.org/10.1084/jem.184.5.1953

Martín-Fontecha, A., S. Sebastiani, U.E. Höpken, M. Uguccioni, M. Lipp, A. Lanzavecchia, and F. Sallusto. 2003. Regulation of dendritic cell migration to the draining lymph node: impact on T lymphocyte traffic and priming. *J. Exp. Med.* 198:615–621. http://dx.doi.org/10.1084/jem.20030448

Martín-Fontecha, A., D. Baumjohann, G. Guarda, A. Reboldi, M. Hons, A. Lanzavecchia, and F. Sallusto. 2008. CD40L+ CD4+ memory T cells migrate in a CD62P-dependent fashion into reactive lymph nodes and license dendritic cells for T cell priming. *J. Exp. Med.* 205:2561–2574. http://dx.doi.org/10.1084/jem.20081212

Menning, A., U.E. Höpken, K. Siegmund, M. Lipp, A. Hamann, and J. Huehn. 2007. Distinctive role of CCR7 in migration and functional activity of naive- and effector/memory-like Treg subsets. *Eur. J. Immunol.* 37:1575–1583. http://dx.doi.org/10.1002/eji.200737201

Meredith, M.M., K. Liu, G. Darrasse-Jeze, A.O. Kamphorst, H.A. Schreiber, P. Guermonprez, J. Idoyaga, C. Cheong, K.H. Yao, R.E. Niec, and M.C. Nussenzweig. 2012. Expression of the zinc finger transcription factor zDC (Zbtb46, Btbd4) defines the classical dendritic cell lineage. *J. Exp. Med.* 209:1153–1165. http://dx.doi.org/10.1084/jem.20112675

Miller, J.C., B.D. Brown, T. Shay, E.L. Gautier, V. Jojic, A. Cohain, G. Pandey, M. Leboeuf, K.G. Elpek, J. Helft, et al. Immunological Genome Consortium. 2012. Deciphering the transcriptional network of the dendritic cell lineage. *Nat. Immunol.* 13:888–899. http://dx.doi.org/10.1038/ni.2370

Mollah, S.A., J.S. Dobrin, R.E. Feder, S.W. Tse, I.G. Matos, C. Cheong, R.M. Steinman, and N. Anandasabapathy. 2014. Flt3L dependence helps define an uncharacterized subset of murine cutaneous dendritic cells. *J. Invest. Dermatol.* 134:1265–1275. http://dx.doi.org/10.1038/jid.2013.515

Naik, S.H., A.I. Proietto, N.S. Wilson, A. Dakic, P. Schnorrer, M. Fuchsberger, M.H. Lahoud, M. O'Keeffe, Q.X. Shao, W.F. Chen, et al. 2005. Cutting edge: generation of splenic CD8+ and CD8- dendritic cell equivalents in Fms-like tyrosine kinase 3 ligand bone marrow cultures. *J. Immunol.* 174:6592–6597. http://dx.doi.org/10.4049/jimmunol.174.11.6592

Noordegraaf, M., V. Flacher, P. Stoitzner, and B.E. Clausen. 2010. Functional redundancy of Langerhans cells and Langerin+ dermal dendritic cells in contact hypersensitivity. *J. Invest. Dermatol.* 130:2752–2759. http://dx.doi.org/10.1038/jid.2010.223

Ohl, L., M. Mohaupt, N. Czeloth, G. Hintzen, Z. Kiafard, J. Zwirner, T. Blankenstein, G. Henning, and R. Förster. 2004. CCR7 governs skin dendritic cell migration under inflammatory and steady-state conditions. *Immunity*. 21:279–288. http://dx.doi.org/10.1016/j.immuni.2004.06.014

Ohnmacht, C., A. Pullner, S.B. King, I. Drexler, S. Meier, T. Brocker, and D. Voehringer. 2009. Constitutive ablation of dendritic cells breaks self-tolerance of CD4 T cells and results in spontaneous fatal autoimmunity. *J. Exp. Med.* 206:549–559. http://dx.doi.org/10.1084/jem.20082394

Pantel, A., C. Cheong, D. Dandamudi, E. Shrestha, S. Mehandru, L. Brane, D. Ruane, A. Teixeira, L. Bozzacco, R.M. Steinman, and M.P. Longhi. 2012. A new synthetic TLR4 agonist, GLA, allows dendritic cells targeted with antigen to elicit Th1 T-cell immunity in vivo. *Eur. J. Immunol.* 42:101–109. http://dx.doi.org/10.1002/eji.201141855

Pepper, M., J.L. Linehan, A.J. Pagán, T. Zell, T. Dileepan, P.P. Cleary, and M.K. Jenkins. 2010. Different routes of bacterial infection induce long-lived TH1 memory cells and short-lived TH17 cells. *Nat. Immunol.* 11:83–89. http://dx.doi.org/10.1038/ni.1826

Petersen, S.H., E. Odintsova, T.A. Haigh, A.B. Rickinson, G.S. Taylor, and F. Berditchevski. 2011. The role of tetraspanin CD63 in antigen presentation via MHC class II. *Eur. J. Immunol.* 41:2556–2561. http://dx.doi.org/10.1002/eji.201141438

Posselt, G., H. Schwarz, A. Duschl, and J. Horejs-Hoeck. 2011. Suppressor of cytokine signaling 2 is a feedback inhibitor of TLR-induced activation in human monocyte-derived dendritic cells. *J. Immunol.* 187:2875–2884. http://dx.doi.org/10.4049/jimmunol.1003348

Romani, N., M. Thurnher, J. Idoyaga, R.M. Steinman, and V. Flacher. 2010. Targeting of antigens to skin dendritic cells: possibilities to enhance vaccine efficacy. *Immunol. Cell Biol.* 88:424–430. http://dx.doi.org/10.1038/icb.2010.39

Sallusto, F., and A. Lanzavecchia. 2009. Heterogeneity of CD4+ memory T cells: functional modules for tailored immunity. *Eur. J. Immunol.* 39:2076–2082. http://dx.doi.org/10.1002/eji.200939722

Sallusto, F., D. Lenig, R. Förster, M. Lipp, and A. Lanzavecchia. 1999. Two subsets of memory T lymphocytes with distinct homing potentials and effector functions. *Nature*. 401:708–712. http://dx.doi.org/10.1038/44385

Sallusto, F., C.R. Mackay, and A. Lanzavecchia. 2000. The role of chemokine receptors in primary, effector, and memory immune responses. *Annu. Rev. Immunol.* 18:593–620. http://dx.doi.org/10.1146/annurev.immunol.18.1.593

Sathaliyawala, T., W.E. O'Gorman, M. Greter, M. Bogunovic, V. Konjufca, Z.E. Hou, G.P. Nolan, M.J. Miller, M. Merad, and B. Reizis. 2010. Mammalian target of rapamycin controls dendritic cell development downstream of Flt3 ligand signaling. *Immunity*. 33:597–606. http://dx.doi.org/10.1016/j.immuni.2010.09.012

Sathe, P., J. Pooley, D. Vremec, J. Mintern, J.O. Jin, L. Wu, J.Y. Kwak, J.A. Villadangos, and K. Shortman. 2011. The acquisition of antigen cross-presentation function by newly formed dendritic cells. *J. Immunol.* 186:5184–5192. http://dx.doi.org/10.4049/jimmunol.1002683

Satpathy, A.T., W. Kc, J.C. Albring, B.T. Edelson, N.M. Kretzer, D. Bhattacharya, T.L. Murphy, and K.M. Murphy. 2012. Zbtb46 expression distinguishes classical dendritic cells and their committed progenitors from other immune lineages. *J. Exp. Med.* 209:1135–1152. http://dx.doi.org/10.1084/jem.20120030

Schulz, O., S.S. Diebold, M. Chen, T.I. Näslund, M.A. Nolte, L. Alexopoulou, Y.T. Azuma, R.A. Flavell, P. Liljeström, and C. Reis e Sousa. 2005. Toll-like receptor 3 promotes cross-priming to virus-infected cells. *Nature*. 433:887–892. http://dx.doi.org/10.1038/nature03326

Shadle, P.J., J.I. Allen, M.D. Geier, and K. Koths. 1989. Detection of endogenous macrophage colony-stimulating factor (M-CSF) in human blood. *Exp. Hematol.* 17:154–159.

Sixt, M., N. Kanazawa, M. Selg, T. Samson, G. Roos, D.P. Reinhardt, R. Pabst, M.B. Lutz, and L. Sorokin. 2005. The conduit system transports soluble antigens from the afferent lymph to resident dendritic cells in the T cell area of the lymph node. *Immunity*. 22:19–29. http://dx.doi.org/10.1016/j.immuni.2004.11.013

Steinman, R.M., D. Hawiger, and M.C. Nussenzweig. 2003. Tolerogenic dendritic cells. *Annu. Rev. Immunol.* 21:685–711. http://dx.doi.org/10.1146/annurev.immunol.21.120601.141040

Travis, M.A., B. Reizis, A.C. Melton, E. Masteller, Q. Tang, J.M. Proctor, Y. Wang, X. Bernstein, X. Huang, L.F. Reichardt, et al. 2007. Loss of integrin $\alpha_{(v)}\beta_8$ on dendritic cells causes autoimmunity and colitis in mice. *Nature*. 449:361–365. http://dx.doi.org/10.1038/nature06110

Trumpfheller, C., M. Caskey, G. Nchinda, M.P. Longhi, O. Mizenina, Y. Huang, S.J. Schlesinger, M. Colonna, and R.M. Steinman. 2008. The microbial mimic poly IC induces durable and protective $CD4^+$ T cell immunity together with a dendritic cell targeted vaccine. *Proc. Natl. Acad. Sci. USA*. 105:2574–2579. http://dx.doi.org/10.1073/pnas.0711976105

Urban, B.C., D.J. Ferguson, A. Pain, N. Willcox, M. Plebanski, J.M. Austyn, and D.J. Roberts. 1999. Plasmodium falciparum-infected erythrocytes modulate the maturation of dendritic cells. *Nature*. 400:73–77. http://dx.doi.org/10.1038/21900

Urban, B.C., N. Willcox, and D.J. Roberts. 2001. A role for CD36 in the regulation of dendritic cell function. *Proc. Natl. Acad. Sci. USA*. 98:8750–8755. http://dx.doi.org/10.1073/pnas.151028698

Waskow, C., K. Liu, G. Darrasse-Jèze, P. Guermonprez, F. Ginhoux, M. Merad, T. Shengelia, K. Yao, and M. Nussenzweig. 2008. The receptor tyrosine kinase Flt3 is required for dendritic cell development in peripheral lymphoid tissues. *Nat. Immunol.* 9:676–683. http://dx.doi.org/10.1038/ni.1615

Zaft, T., A. Sapoznikov, R. Krauthgamer, D.R. Littman, and S. Jung. 2005. CD11chigh dendritic cell ablation impairs lymphopenia-driven proliferation of naive and memory CD8+ T cells. *J. Immunol.* 175:6428–6435. http://dx.doi.org/10.4049/jimmunol.175.10.6428

Zhang, J.G., P.E. Czabotar, A.N. Policheni, I. Caminschi, S.S. Wan, S. Kitsoulis, K.M. Tullett, A.Y. Robin, R. Brammananth, M.F. van Delft, et al. 2012. The dendritic cell receptor Clec9A binds damaged cells via exposed actin filaments. *Immunity*. 36:646–657. http://dx.doi.org/10.1016/j.immuni.2012.03.009